ELECTRONIC SUPPLEMENTARY INFORMATION

Synthesis of Planar Dibenzo[*de, op*]bistetracene Derivatives for Organic Field-effect Transistors Applications: Substituent Effect on Crystal Packing and Charge Transport Property

Tien-Lin Wu,[1] Chi-Hsien Kuo,[2] Bo-Chao Lin,[2] Yu-Tai Tao[1,2,*] Chao-Ping Hsu,[2,*] and Rai-Shung Liu[1,*]

[1]Department of Chemistry, National Tsing Hua University, Hsin-Chu, Taiwan

[2]Institute of Chemistry, Academia Sinica, Taipei, Taiwan

E-mail: ytt@gate.sinica.edu.tw, cherri@sinica.edu.tw, rsliu@mx.nthu.edu.tw

Table of Contents:

(A) Synthetic procedure and analytic data……...S2
(B) X-ray crystallographic analysis data……S11
(C) Output characteristics and transfer characteristics……..…….S16
(D) NMR spectra.....…….....S18
(E) HRMS mass spectra for key compounds **4a-4d**……..….....S40
(F) Computational details……S42

(A) Synthetic procedure and analytic data

(1) Experimental Procedures for the Synthesis of 4a

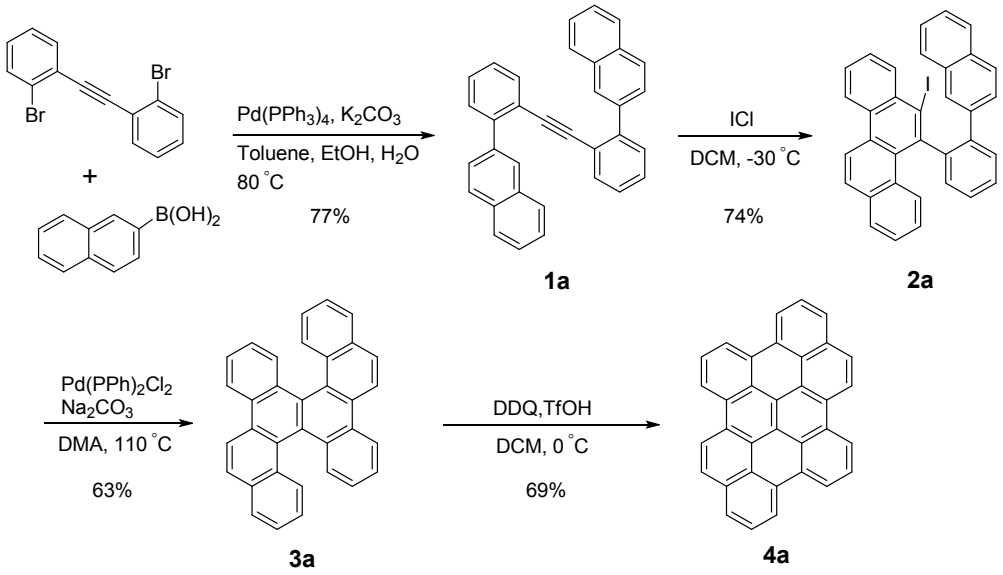

Synthesis of compound 1a

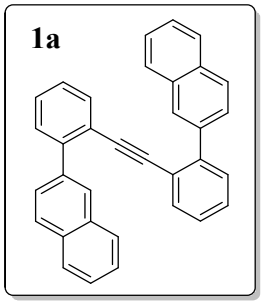

Nitrogen was bubbled through a mixed solution of toluene (160 mL), EtOH (40 mL) and water (40 mL) for 30 min, and to this solution were added compound 1,2-bis(2-bromophenyl)ethyne (2.80 g, 8.33 mmol), $Pd(PPh_3)_4$ (390 mg, 0.33 mmol), K_2CO_3 (6.91 g, 50.0 mmol) and naphthalen-2-ylboronic acid (2.97 g, 17.3 mmol). The mixture was heated at 80 °C for 24 h. The solution was extracted with dichloromethane, concentrated and purified on a silica gel column chromatograph (dichloromethane/hexane = 1/10) to afford compound **1a** (2.76 g, 6.41 mmol, 77 %) as a white solid. ^{1}H NMR (400 MHz, $CDCl_3$): δ 7.99 (s, 2H), 7.80-7.77 (m, 4H), 7.67 (s, 4H), 7.47-7.33 (m, 10H), 7.22 (t, J = 7.4 Hz, 2H). ^{13}C NMR (100 MHz, $CDCl_3$): δ 143.3, 137.9, 133.1, 132.6, 129.7, 128.5, 128.2, 128.1, 127.6, 127.6, 127.6, 127.1, 127.0, 126.0, 126.0, 121.9, 92.2. HRMS Calcd for $C_{34}H_{22}$: 430.1722. Found: 430.1729.

Synthesis of compound 2a

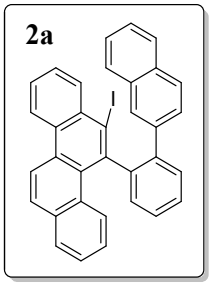

A solution of compound **1a** (2.08 g, 4.82 mmol) in dry CH_2Cl_2 (480 mL) was maintained at -30 °C under a argon atmosphere. To this solution was added ICl (6.27 mL, 1 M solution in CH_2Cl_2), using a standard syringe. The reaction was stirred for 3 h before quenched with a saturated sodium sulfite solution. The solution was extracted with CH_2Cl_2 (2×20 mL) and dried over $MgSO_4$. After concentrated under reduced pressure, the crude material was purified by column chromatography (dichloromethane/hexane = 1/10) to afford compound **2a** (1.98 g, 3.57 mmol, 74 %) as a yellow oil. ^{1}H NMR (400 MHz, $CDCl_3$): δ 8.59 (d, *J* = 7.9 Hz, 1H), 8.53 (d, *J* = 9.1 Hz, 1H), 8.38 (dd, *J* = 1.1, 7.9 Hz, 1H), 7.83-7.81 (m, 2H), 7.74 (d, *J* = 8.5 Hz, 1H), 7.68-7.55 (m, 5H), 7.51-7.41 (m, 3H), 7.32-7.29 (m, 2H), 7.26-7.15 (m, 4H), 7.05 (dd, *J* = 1.6, 8.5 Hz, 1H). ^{13}C NMR (100 MHz, $CDCl_3$): δ 147.9, 143.3, 141.1, 138.2, 134.8, 133.5, 133.2, 132.7, 131.9, 131.8, 131.3, 130.5, 130.2, 129.9, 129.3, 128.8, 128.7, 128.4, 128.2, 128.0, 127.9, 127.9, 127.8, 127.3, 127.1, 126.7, 126.6, 125.9, 125.5, 125.4, 125.4, 123.3, 121.0, 111.6. HRMS Calcd for $C_{34}H_{21}I$: 556.0688. Found: 556.0696.

Synthesis of compound 3a

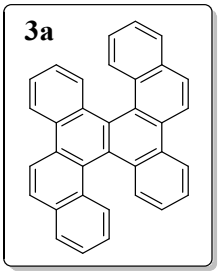

A two-neck round bottom flask was charged with **2a** (283 mg, 0.51 mmol), Pd $(PPh_3)_2Cl_2$ (29 mg, 0.025 mmol), and Na_2CO_3 (216 mg, 2.04 mmol) under a argon atmosphere, and to this mixture was added N,N-dimethylacetamide (DMA, 51 mL). The resulting solution was heated at 110 °C for 12 h, cooled to room temperature, and the solution was extracted with ethyl acetate (3×30 mL), After concentrated under reduced pressure, the crude material was purified by column chromatography (dichloromethane/hexane = 1/10) to afford compound

3a (138 mg, 0.32 mmol, 63%) as a yellow solid. ^{1}H NMR (400 MHz, CD_2Cl_2): δ 8.80 (d, *J* = 9.0 Hz, 2H), 8.73-8.71 (m, 2H), 8.39 (d, *J* = 8.5 Hz, 2H), 8.18 (d, *J* = 8.8 Hz, 2H), 8.13-8.11 (m, 2H), 8.03 (d, *J* = 8.2 Hz, 2H), 7.60-7.51 (m, 4H), 7.32-7.27 (m, 4H). ^{13}C NMR (100 MHz, $CDCl_3$): δ 132.7, 131.8, 130.8, 129.7, 129.3, 129.1, 129.1, 128.9, 128.1, 128.1, 128.1, 126.5, 126.0, 126.0, 125.2, 123.4, 121.0. HRMS Calcd for $C_{34}H_{20}$: 428.1565. Found: 428.1563.

Synthesis of compound 4a

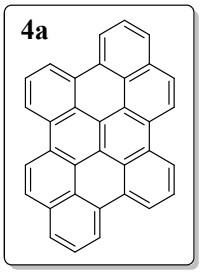

To a mixture of **3a** (240 mg, 0.56 mmol) and DDQ (267 mg, 1.18 mmol) in dry CH_2Cl_2 (56 mL) at 0 °C under a argon atmosphere was added trifluoromethanesulfonic acid (5.6 mL). After 3 h, the resulting mixture was quenched by saturated $NaHCO_3$ solution (150 mL), and filter it. The crude material were washed with DI water and ethyl acetate. After removal of solvent in vacuo, the crude material was purified by vacuum sublimation to afford compound **4a** (164 mg, 0.39 mmol, 69%) as light orange solid. The pure product was insoluble in d-chloroform, d2-dichloromethane and other d-solvents. HRMS Calcd for $C_{34}H_{16}$: 424.1252. Found: 424.1259.

(2) Experimental Procedures for the Synthesis of 4b

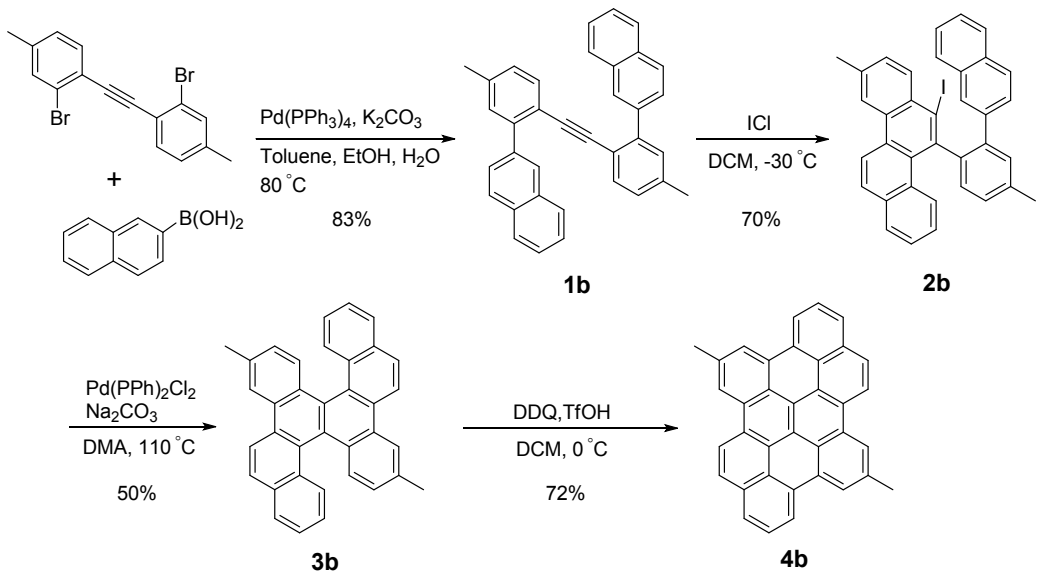

Synthesis of compound 1b

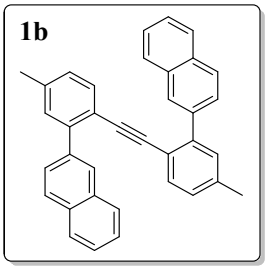

Compound **1b** was prepared similarly from 1,2-bis(2-bromo-4-methylphenyl)ethyne (3.16 g, 8.67 mmol), affording a yellow solid (3.30 g, 7.20 mmol, 83 %). 1H NMR (400 MHz, $CDCl_3$): δ 7.98 (s, 4=2H), 7.79-7.75 (m, 4H), 7.68-7.62 (m, 4H), 7.47-7.43 (m, 4H), 7.27-7.25 (m, 4H), 7.03 (dd, J = 1.4, 7.8 Hz, 2H), 2.37 (s, 6H). 13C NMR (100 MHz, CDCl3): δ 143.0, 138.4, 138.1, 133.2, 133.0, 132.6, 130.4, 128.14, 128.0, 127.9, 127.6, 127.6, 127.0, 125.9, 125.9, 119.1, 91.6, 21.5. HRMS Calcd for C36H26: 458.2035. Found: 458.2040.

Synthesis of compound 2b

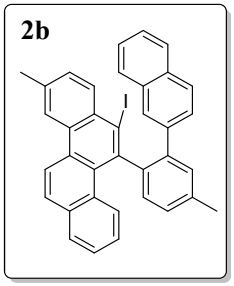

Compound **2b** was prepared similarly from **1b** (1.87 g, 4.07 mmol), affording a yellow oil (1.67 g, 2.85 mmol, 70 %). ^{1}H NMR (400 MHz, $CDCl_3$): δ 8.51 (d, *J* = 9.2 Hz, 1H), 8.37 (s, 1H), 8.24 (d, *J* = 8.5 Hz, 1H), 7.82-7.77 (m, 3H), 7.50-7.36 (m, 5H), 7.30-7.28 (m, 3H), 7.25-7.15 (m, 4H), 7.02 (dd, *J* = 1.8, 8.5 Hz, 1H), 2.60 (s, 3H), 2.59 (s, 3H). ^{13}C NMR (100 MHz, $CDCl_3$): δ 145.1, 142.3, 140.9, 138.4, 138.4, 137.0, 134.6, 133.5, 132.7, 132.0, 131.8, 131.7, 131.4, 130.7, 130.2, 129.6, 129.5, 129.5, 128.9, 128.5, 128.3, 128.1, 127.9, 127.7, 127.1, 126.8, 126.5, 125.7, 125.3, 125.3, 125.3, 122.8, 121.1, 111.8, 21.8, 21.6. HRMS Calcd for $C_{36}H_{25}I$: 584.1001. Found: 584.1002.

Synthesis of compound 3b

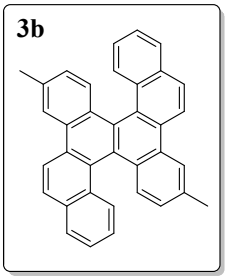

Compound **3b** was prepared similarly from **2b** (314 mg, 0.54 mmol), affording a yellow powder (158 mg, 0.27 mmol, 50 %). ^{1}H NMR (400 MHz, CD_2Cl_2): δ 8.78 (d, *J* = 9.0 Hz, 2H), 8.50 (s, 2H), 8.40 (d, *J* = 8.6 Hz, 2H), 8.15 (d, *J* = 8.8 Hz, 2H), 8.02-7.98 (m, 4H), 7.53-7.49 (m, 2H), 7.30-7.25 (m, 2H), 7.13 (dd, *J* = 1.3, 8.6 Hz, 2H), 2.58 (s, 6H). ^{13}C NMR (100 MHz, $CDCl_3$): δ 136.1, 132.7, 130.9, 129.8, 129.7, 129.1, 129.1, 128.9, 128.3, 128.1, 127.8, 127.5, 125.9, 125.4, 125.1, 123.1, 121.1, 21.8. HRMS Calcd for $C_{36}H_{24}$: 456.1878. Found: 456.1875.

Synthesis of compound 4b

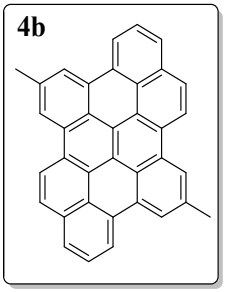

Compound **4b** was prepared similarly from **3b** (363 mg, 0.80 mmol), affording an orange powder (261 mg, 0.58 mmol, 72 %). The pure product was insoluble in d-chloroform, d_2-dichloromethane and other d-solvents. HRMS Calcd for $C_{36}H_{20}$: 452.1565. Found: 452.1572.

(3) Experimental Procedures for the Synthesis of 4c

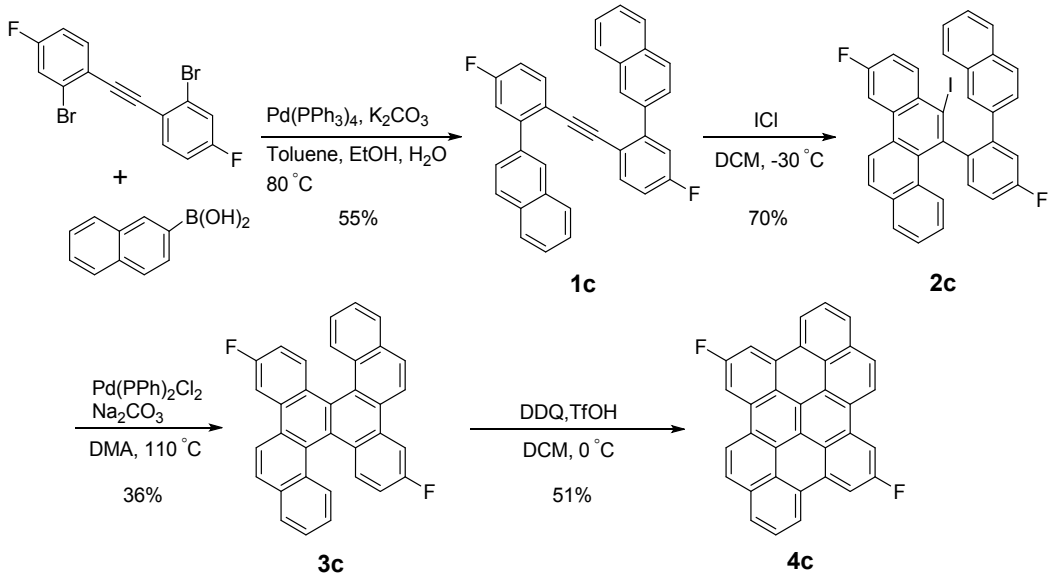

Synthesis of compound 1c

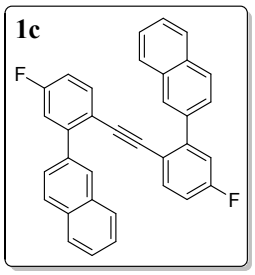

Compound **1c** was prepared similarly from 1,2-bis(2-bromo-4-fluorophenyl)ethyne (1.43 g, 3.84 mmol), affording a yellow solid (985 mg, 2.11 mmol, 55 %). ^{1}H NMR (400 MHz, $CDCl_3$): δ 7.96 (s, 4=2H), 7.80-7.75 (m, 4H), 7.67-7.60 (m, 4H), 7.50-7.45 (m, 4H), 7.31 (dd, J = 5.8, 8.6 Hz, 2H), 7.15 (dd, J = 2.6, 9.6 Hz, 2H), 6.92 (td, J = 2.6, 8.2 Hz, 2H). ^{13}C NMR (100 MHz, $CDCl_3$): δ 162.4 (d, J = 248 Hz), 145.6 (d, J = 8 Hz), 136.8, 134.8 (d, J = 8 Hz), 133.0, 132.8, 128.2, 128.1, 127.7, 127.4, 127.0, 126.3, 126.2, 117.8, 116.7 (d, J = 22 Hz), 114.3 (d, J = 22 Hz), 90.7. HRMS Calcd for $C_{34}H_{20}F_2$: 466.1533. Found: 466.1532.

Synthesis of compound 2c

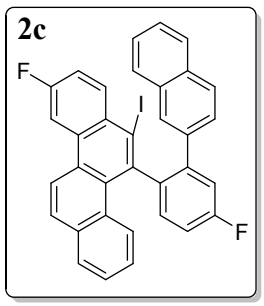

Compound **2c** was prepared similarly from **1c** (977 mg, 2.09 mmol), affording a yellow oil (868 mg, 1.47 mmol, 70 %). ^{1}H NMR (400 MHz, CD_2Cl_2): δ 8.44-8.38 (m, 1H), 8.35 (d, *J* = 9.1 Hz, 1H), 8.25 (dd, *J* = 2.5, 11.4 Hz, 1H), 7.87-7.83 (m, 2H), 7.76 (d, *J* = 8.8 Hz, 1H), 7.54-7.51 (m, 2H), 7.44-7.22 (m, 10H), 6.99 (dd, *J* = 1.8, 8.6 Hz, 1H). ^{13}C NMR (100 MHz, $CDCl_3$): δ 163.6 (d, *J* = 90 Hz), 161.1 (d, *J* = 90 Hz), 143.7, 143.7, 143.2 (d, *J* = 8 Hz), 141.6, 141.5, 137.5 (d, *J* = 9 Hz), 136.9, 136.9, 133.7, 133.5 (d, *J* = 8 Hz), 132.5, 132.0, 131.3 (d, *J* = 8 Hz), 130.2, 128.9, 128.5, 127.9, 127.8, 127.8, 127.1, 126.8, 126.2, 126.1, 125.7, 125.7, 125.6, 120.8, 118.0 (d, *J* = 22 Hz), 117.0 (d, *J* = 24 Hz), 115.2 (d, *J* = 21 Hz), 111.0, 107.8 (d, *J* = 23 Hz). HRMS Calcd for $C_{34}H_{19}F_2I$: 592.0500. Found: 592.0507.

Synthesis of compound 3c

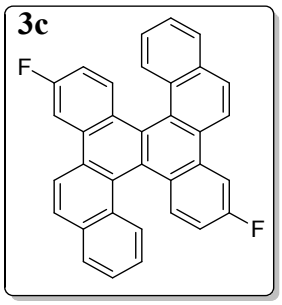

Compound **3c** was prepared similarly from **2c** (484 mg, 0.82 mmol), affording a yellow powder (137 mg, 0.30 mmol, 36 %). ^{1}H NMR (400 MHz, $CDCl_3$): δ 8.59 (d, *J* = 8.9 Hz, 2H), 8.35 (d, *J* = 8.6 Hz, 2H), 8.27 (dd, *J* = 2.6, 10.8 Hz, 2H), 8.12 (d, *J* = 9.0 Hz, 2H), 8.11 (d, *J* = 9.2 Hz, 2H), 8.35 (d, *J* = 8.0 Hz, 2H), 7.54-7.50 (m, 2H), 7.31-7.27 (m, 2H), 7.04-6.99 (m, 2H). ^{13}C NMR (100 MHz, $CDCl_3$): δ 161.4 (d, *J* = 245 Hz), 133.0, 131.5 (d, *J* = 8 Hz), 130.8 (d, *J* = 8 Hz), 130.6, 129.5, 128.5, 128.5, 128.4, 128.3, 127.8, 126.5, 125.6, 125.5, 120.9, 114.7 (d, *J* = 23 Hz), 108.5 (d, *J* = 23 Hz). HRMS Calcd for $C_{34}H_{18}F_2$: 464.1377. Found: 464.1380.

Synthesis of compound 4c

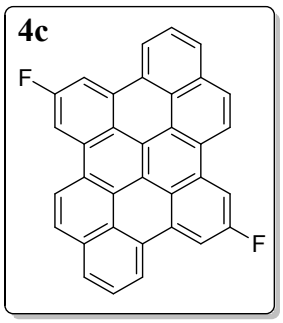

Compound **4c** was prepared similarly from **3c** (330 mg, 0.71 mmol), affording a deep orange powder (167 mg, 0.36 mmol, 51 %). The pure product was insoluble in d-chloroform, d_2-dichloromethane and other d-solvents. HRMS Calcd for $C_{34}H_{14}F_2$: 460.1064. Found: 460.1057.

(4) Experimental Procedures for the Synthesis of 4d

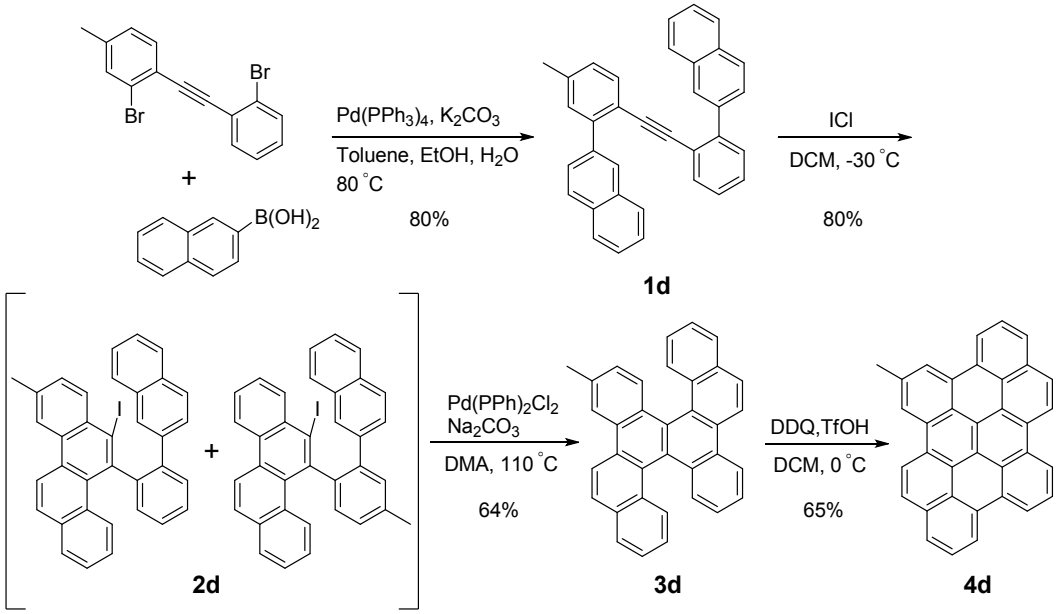

Synthesis of compound 1d

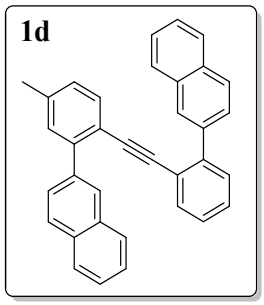

Compound **1d** was prepared similarly from 2-bromo-1-((2-bromophenyl)ethynyl)-4-methylbenzene (1.71 g, 4.89 mmol), affording a yellow solid (1.74 g, 3.91 mmol, 80 %). ^{1}H NMR (400 MHz, $CDCl_3$): δ 8.07 (s, 1H), 8.06 (s, 1H), 7.86-7.83 (m, 4H), 7.77-.7.71 (m, 4H), 7.54-7.44 (m, 6H), 7.40-7.24 (m, 4H), 7.09 (dd, *J* = 1.0, 7.9 Hz, 1H), 2.41 (s, 3H). ^{13}C NMR (100 MHz, $CDCl_3$): δ 143.1, 138.6, 138.0, 138.0, 133.1, 133.1, 133.0, 133.0, 133.0, 132.6, 130.4, 129.6, 128.2, 128.1, 128.1, 128.0, 128.0, 127.9, 127.6, 127.6, 127.6, 127.6, 127.6, 127.1, 127.1, 127.0, 125.9, 125.9, 125.9, 125.9, 122.0, 118.9, 92.4, 91.5, 21.4. HRMS Calcd for $C_{35}H_{24}$: 444.1878. Found: 444.1880.

Synthesis of compound 2d

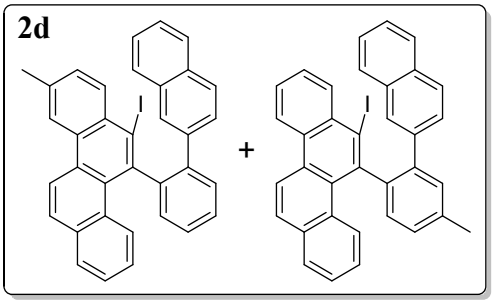

Compound **2d** was prepared similarly from **1d** (1.65 g, 3.70 mmol), affording two inseparable stereoisomers (1.69 g, 2.96 mmol, 80 %) and directly using in the next step without further purification.

Synthesis of compound 3d

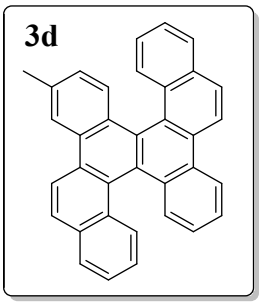

Compound **3d** was prepared similarly from **2d** (1.31 g, 2.30 mmol), affording a yellow oil (651 mg, 1.47 mmol, 64 %). 1H NMR (400 MHz, CDCl3): δ 8.74 (d, J = 8.9 Hz, 2H), 8.66 (dd, J = 0.6, 8.2 Hz, 2H), 8.45 (s, 1H), 8.41 (t, J = 8.6 Hz, 2H), 8.13-8.09 (m, 3H), 8.03-7.97 (m, 3H), 7.54-7.47 (m, 3H), 7.29-7.25 (m, 3H), 7.10 (dd, J = 1.4, 8.6 Hz, 2H), 2.56 (s, 3H). 13C NMR (100 MHz, CDCl3): δ 136.4, 136.4, 132.7, 132.7, 131.8, 130.9, 130.9, 129.8, 129.7, 129.3, 129.2, 129.2, 129.1, 129.0, 128.9, 128.9, 128.2, 128.1, 128.1, 128.0, 127.9, 127.6, 126.3, 125.9, 125.9, 125.9, 125.4, 125.2, 125.2, 125.2, 123.3, 123.2, 121.0, 121.0, 21.8. HRMS Calcd for $C_{35}H_{22}$: 442.1722. Found: 442.1724.

Synthesis of compound 4d

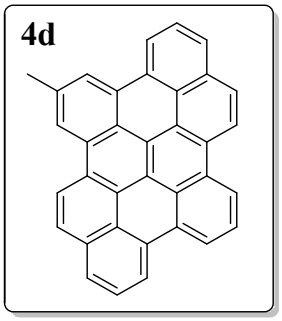

Compound **4d** was prepared similarly from **3d** (790 mg, 1.79 mmol), affording an orange powder (510 mg, 1.16 mmol, 65 %). The pure product was insoluble in d-chloroform, d_2-dichloromethane and other d-solvents. HRMS Calcd for C35H18: 438.1409. Found: 438.1409.

(5) Experimental Procedures for the Synthesis of 4e

The compound **4e** was prepared from 1,2-bis(2-bromo-4-*tert*-butyl)ethyne according to a literature procedure.[1]

Reference:

1. T.-A. Chen, R.-S. Liu, *Org. Lett.* 2011, **13**, 4644−4647.

(B) X-ray crystallographic analysis data

Table SB1. Experimental details for X-ray crystal structure **4a**

Crystal data	**4a**
Empirical formula	$C_{17}H_8$
Formula weight	212.23
Temperature	200(2) K
Wavelength	0.71073 Å
Crystal system	Monoclinic
Space group	P 2_1/c
***a*, *b*, *c* (Å)**	11.5659(4) , 5.13300(10), 15.5436(5)
α, β, γ (°)	90, 90.063(2), 90

Volume	922.79(5) Å^3
Z	4
Density (calculated)	1.528 Mg/m^3
Absorption coefficient	0.087 mm^{-1}
F(000)	440
Crystal size	0.84 × 0.13 × 0.11 mm^3
Theta range for data collection	1.76 to 26.37°
Index ranges	-14<=h<=14, -6<=k<=6, -19<=l<=19
Reflections collected	22871
Independent reflections	1892 [R(int) = 0.0402]
Completeness to theta = 25.00°	100.0 %
Absorption correction	Semi-empirical from equivalents
Max. and min. transmission	0.9905 and 0.9306
Refinement method	Full-matrix least-squares on F^2
Data / restraints / parameters	1892 / 49 / 154
Goodness-of-fit on F^2	1.086
Final R indices [I>2sigma(I)]	R1 = 0.0483, wR2 = 0.1263
R indices (all data)	R1 = 0.0691, wR2 = 0.1419
Largest diff. peak and hole	0.366 and -0.217 e.Å^{-3}

Table SB2. Experimental details for X-ray crystal structure **4b**

Crystal data	**4b**
Empirical formula	$C_{36}H_{20}$
Formula weight	452.52
Temperature	200(2) K
Wavelength	0.71073 Å
Crystal system	Orthorhombic
Space group	P bca
***a*, *b*, *c* (Å)**	5.0661(17) , 15.948(6), 25.586(9)
α, β, γ (°)	90, 90, 90
Volume	2067.2(12) Å^3
Z	4
Density (calculated)	1.454 Mg/m^3
Absorption coefficient	0.083 mm^{-1}

F(000)	944
Crystal size	0.79 × 0.06 × 0.02 mm^3
Theta range for data collection	1.59 to 25.04°
Index ranges	-6<=h<=4, -18<=k<=18, -30<=l<=30
Reflections collected	13633
Independent reflections	1795 [R(int) = 0.1562]
Completeness to theta = 25.04°	98.9 %
Absorption correction	multi-scan
Max. and min. transmission	0.9984 and 0.9377
Refinement method	Full-matrix least-squares on F^2
Data / restraints / parameters	1795 / 0 / 163
Goodness-of-fit on F^2	1.016
Final R indices [I>2sigma(I)]	R1 = 0.0659, wR2 = 0.1682
R indices (all data)	R1 = 0.1674, wR2 = 0.2555
Largest diff. peak and hole	0.478 and -0.476 e.$Å^{-3}$

Table SB3. Experimental details for X-ray crystal structure **4c**

Crystal data	**4c**
Empirical formula	$C_{17}H_7F$
Formula weight	230.23
Temperature	100.00(10) K
Wavelength	0.71073 Å
Crystal system	Monoclinic
Space group	P $2_1/c$
***a*, *b*, *c* (Å)**	11.8364(4) , 5.0807(2), 15.5746(6)
α, β, γ (°)	90, 90.487(2), 90
Volume	936.58(6) $Å^3$
Z	4
Density (calculated)	1.633 Mg/m^3
Absorption coefficient	0.107 mm^{-1}
F(000)	472
Crystal size	0.58 × 0.3 × 0.17 mm^3
Theta range for data collection	1.72 to 27.1°
Index ranges	-15<=h<=15, -6<=k<=6, -19<=l<=19
Reflections collected	17821

Independent reflections	2057 [R(int) = 0.0403]
Completeness to theta = 25.00°	100.0 %
Absorption correction	Semi-empirical from equivalents
Max. and min. transmission	0.982 and 0.9404
Refinement method	Full-matrix least-squares on F^2
Data / restraints / parameters	2057 / 0 / 163
Goodness-of-fit on F^2	1.047
Final R indices [I>2sigma(I)]	R1 = 0.0394, wR2 = 0.1075
R indices (all data)	R1 = 0.0567, wR2 = 0.1215
Largest diff. peak and hole	0.309 and -0.217 e.$Å^{-3}$

Table SB4. Experimental details for X-ray crystal structure **4d**

Crystal data	**4d**
Empirical formula	$C_{35}H_{18}$
Formula weight	212.23
Temperature	296(2) K
Wavelength	0.71073 Å
Crystal system	Monoclinic
Space group	P 2_1/c
***a*, *b*, *c* (Å)**	12.403(6) , 5.099(2), 15.999(7)
α, β, γ (°)	90, 95.079(14), 90
Volume	1007.8(7) $Å^3$
Z	2
Density (calculated)	1.445 Mg/m^3
Absorption coefficient	0.082 mm^{-1}
F(000)	456
Crystal size	0.79 × 0.05 × 0.02 mm^3
Theta range for data collection	1.65 to 25.04°
Index ranges	-14<=h<=14, -5<=k<=2, -18<=l<=12
Reflections collected	4017
Independent reflections	1746 [R(int) = 0.0586]
Completeness to theta = 25.04°	98.6 %
Absorption correction	Semi-empirical from equivalents
Max. and min. transmission	0.9984 and 0.9380
Refinement method	Full-matrix least-squares on F^2

Data / restraints / parameters	1746 / 0 / 164
Goodness-of-fit on F^2	0.919
Final R indices [I>2sigma(I)]	R1 = 0.0780, wR2 = 0.2024
R indices (all data)	R1 = 0.2131, wR2 = 0.2964
Largest diff. peak and hole	0.350 and -0.404 e.Å^{-3}

Table SB5. Experimental details for X-ray crystal structure **4e**

Crystal data	**4e**
Empirical formula	$C_{42}H_{32}$
Formula weight	536.68
Temperature	200(2) K
Wavelength	0.71073 Å
Crystal system	Monoclinic
Space group	C 2/c
***a*, *b*, *c* (Å)**	26.659(4) , 6.1038(11), 19.317(4)
α, β, γ (°)	90, 90.063(2), 90
Volume	922.79(5) Å^3
Z	4
Density (calculated)	1.299 Mg/m^3
Absorption coefficient	0.073 mm^{-1}
F(000)	1136
Crystal size	0.68 × 0.04 × 0.01 mm^3
Theta range for data collection	1.75 to 25.06°
Index ranges	-31<=h<=30, -7<=k<=7, -22<=l<=22
Reflections collected	8616
Independent reflections	2427 [R(int) = 0.1070]
Completeness to theta = 25.06°	99.6 %
Absorption correction	Semi-empirical from equivalents
Max. and min. transmission	0.9993 and 0.9519
Refinement method	Full-matrix least-squares on F^2
Data / restraints / parameters	2427 / 0 / 190
Goodness-of-fit on F^2	0.952
Final R indices [I>2sigma(I)]	R1 = 0.0680, wR2 = 0.1624
R indices (all data)	R1 = 0.2130, wR2 = 0.2590
Largest diff. peak and hole	0.608 and -0.572 e.Å^{-3}

(C) Output characteristics and transfer characteristics

Figure SC1

(a) Output characteristics and (b) transfer characteristics of **4a**

(c) Output characteristics and (d) transfer characteristics of **4b**

(e) Output characteristics and (f) transfer characteristics of **4c**

(g) Output characteristics and (h) transfer characteristics of **4d**

(i) Output characteristics and (j) transfer characteristics of **4e**

(a) **(b)**

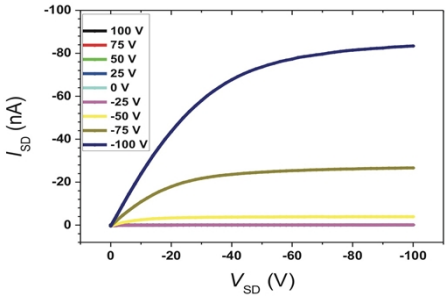

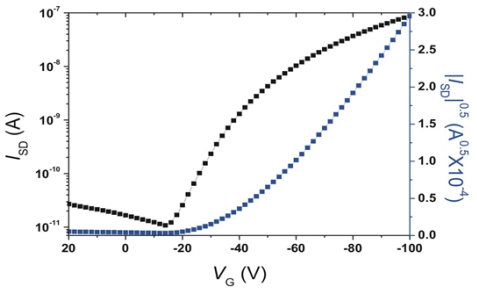

(c) **(d)**

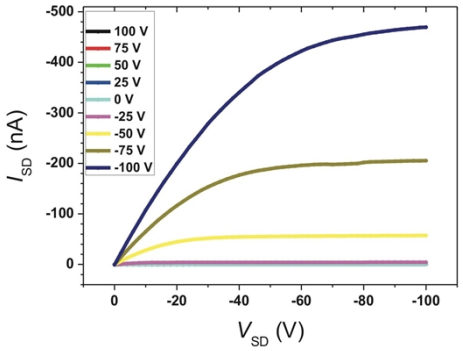

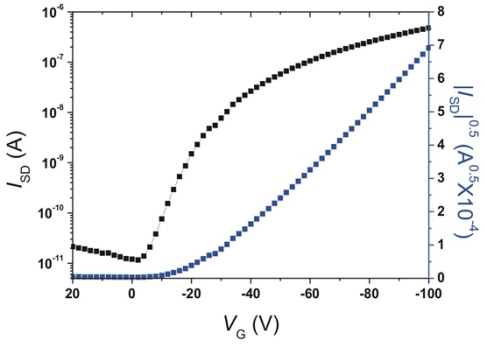

(e) **(f)**

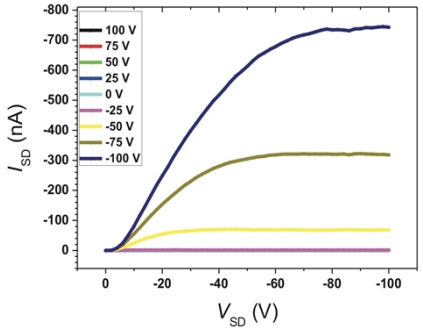
100 V
75 V
50 V
25 V
0 V
-25 V
-50 V
-75 V
-100 V
I_{SD} (nA)
V_{SD} (V)

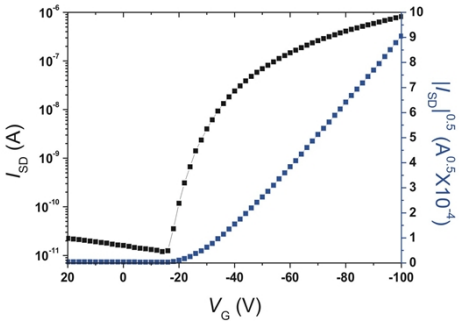
I_{SD} (A)
$|I_{SD}|^{0.5}$ ($A^{0.5}X10^{-4}$)
V_G (V)

(g) **(h)**

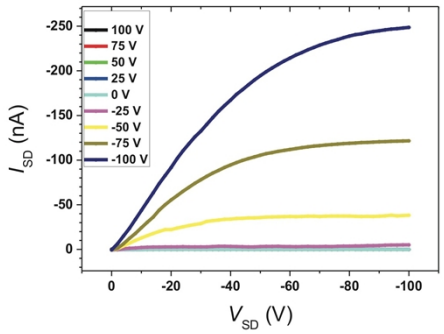
100 V
75 V
50 V
25 V
0 V
-25 V
-50 V
-75 V
-100 V
I_{SD} (nA)
V_{SD} (V)

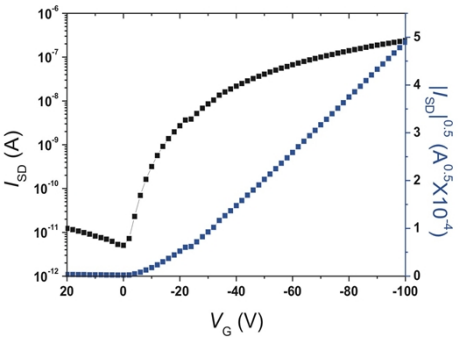
I_{SD} (A)
$|I_{SD}|^{0.5}$ ($A^{0.5}X10^{-4}$)
V_G (V)

(i) **(j)**

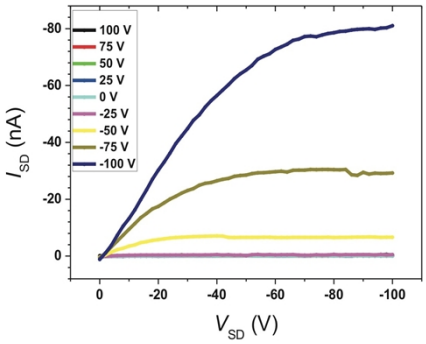
100 V
75 V
50 V
25 V
0 V
-25 V
-50 V
-75 V
-100 V
I_{SD} (nA)
V_{SD} (V)

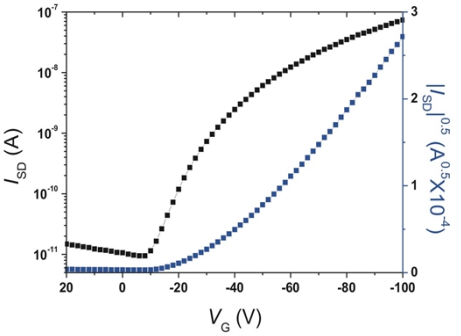
I_{SD} (A)
$|I_{SD}|^{0.5}$ ($A^{0.5}X10^{-4}$)
V_G (V)

(D) NMR spectra

^{1}H NMR of Compound **1a**

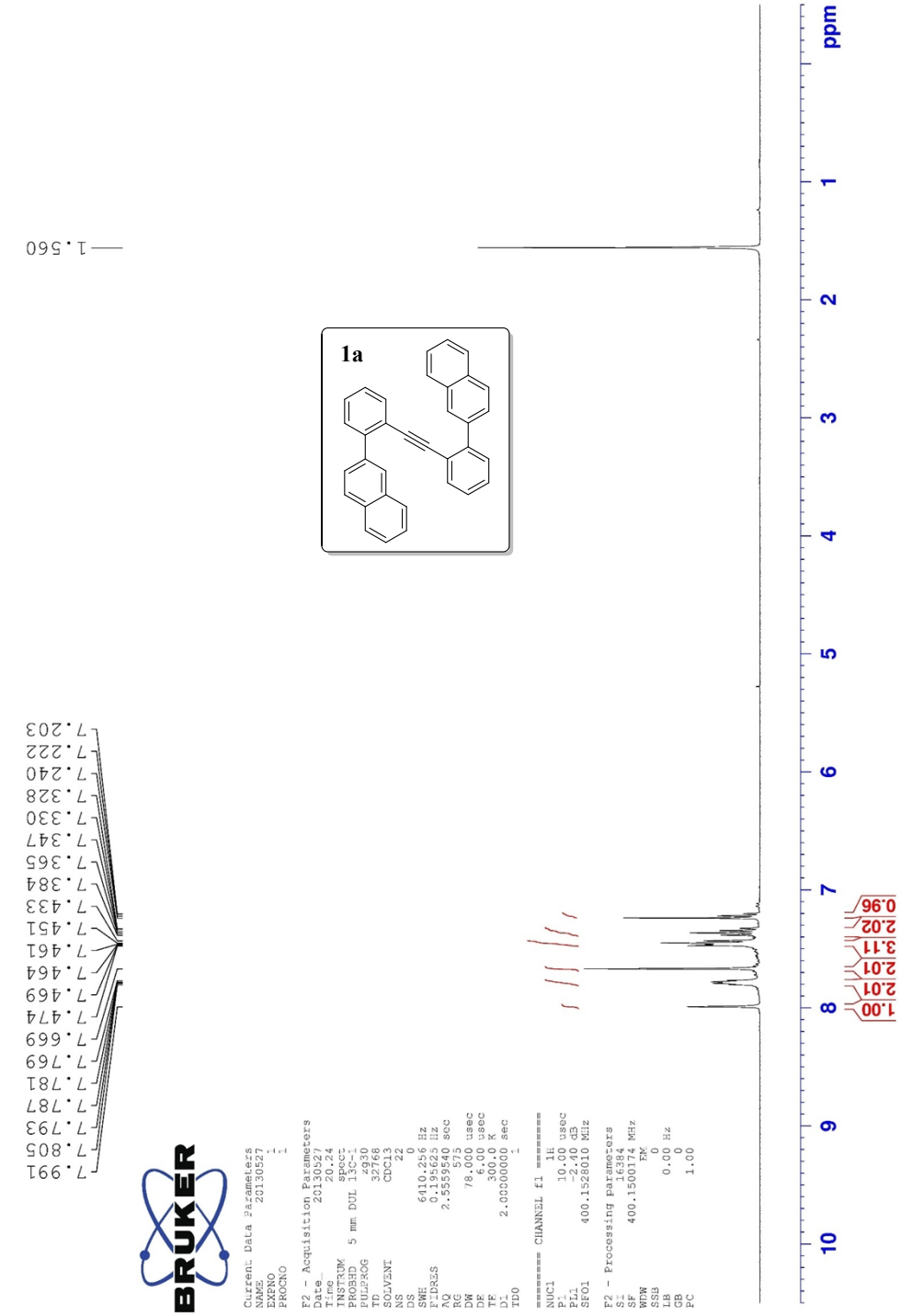

^{13}C NMR and DEPT of Compound **1a**

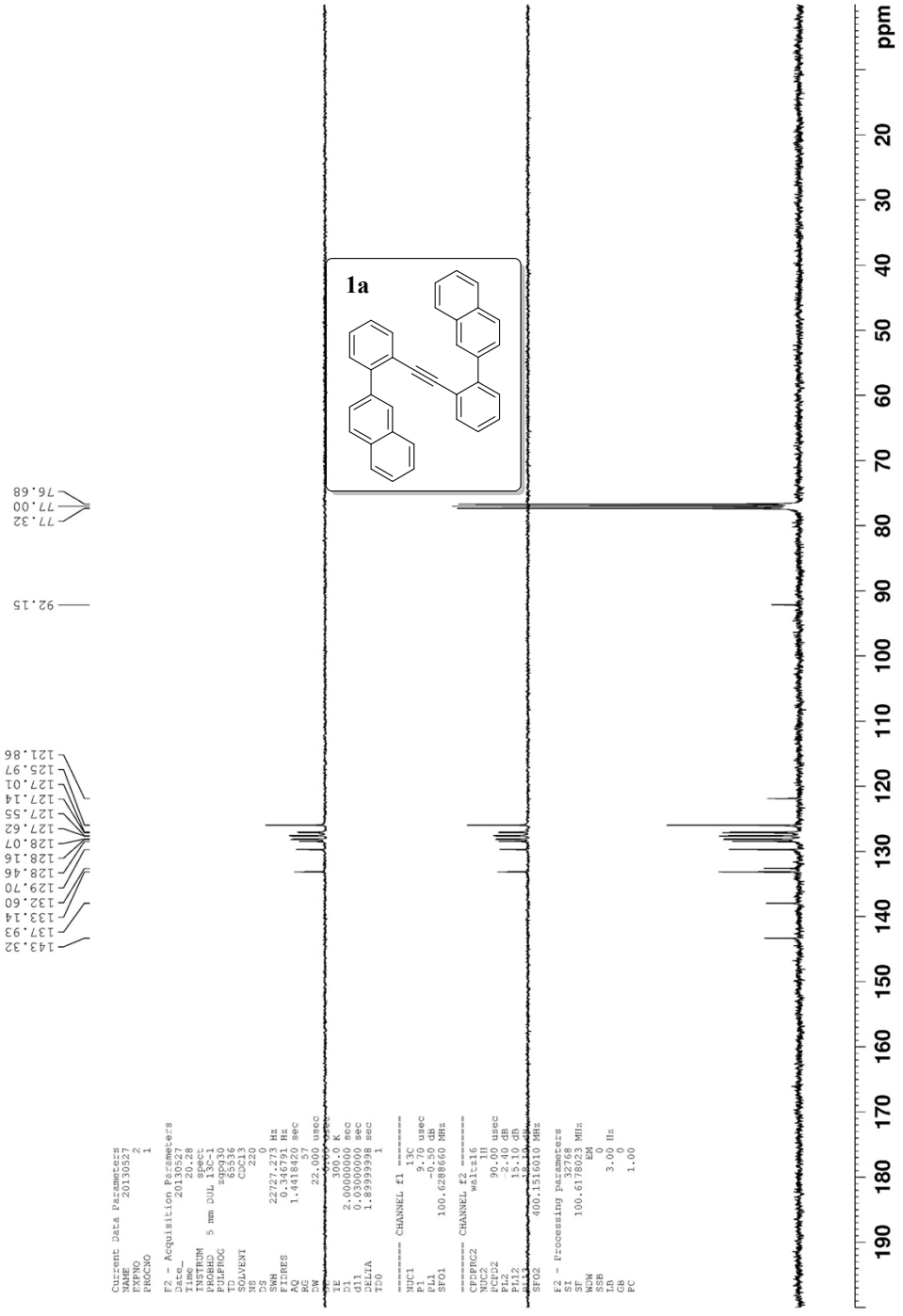

^{1}H NMR of Compound **2a**

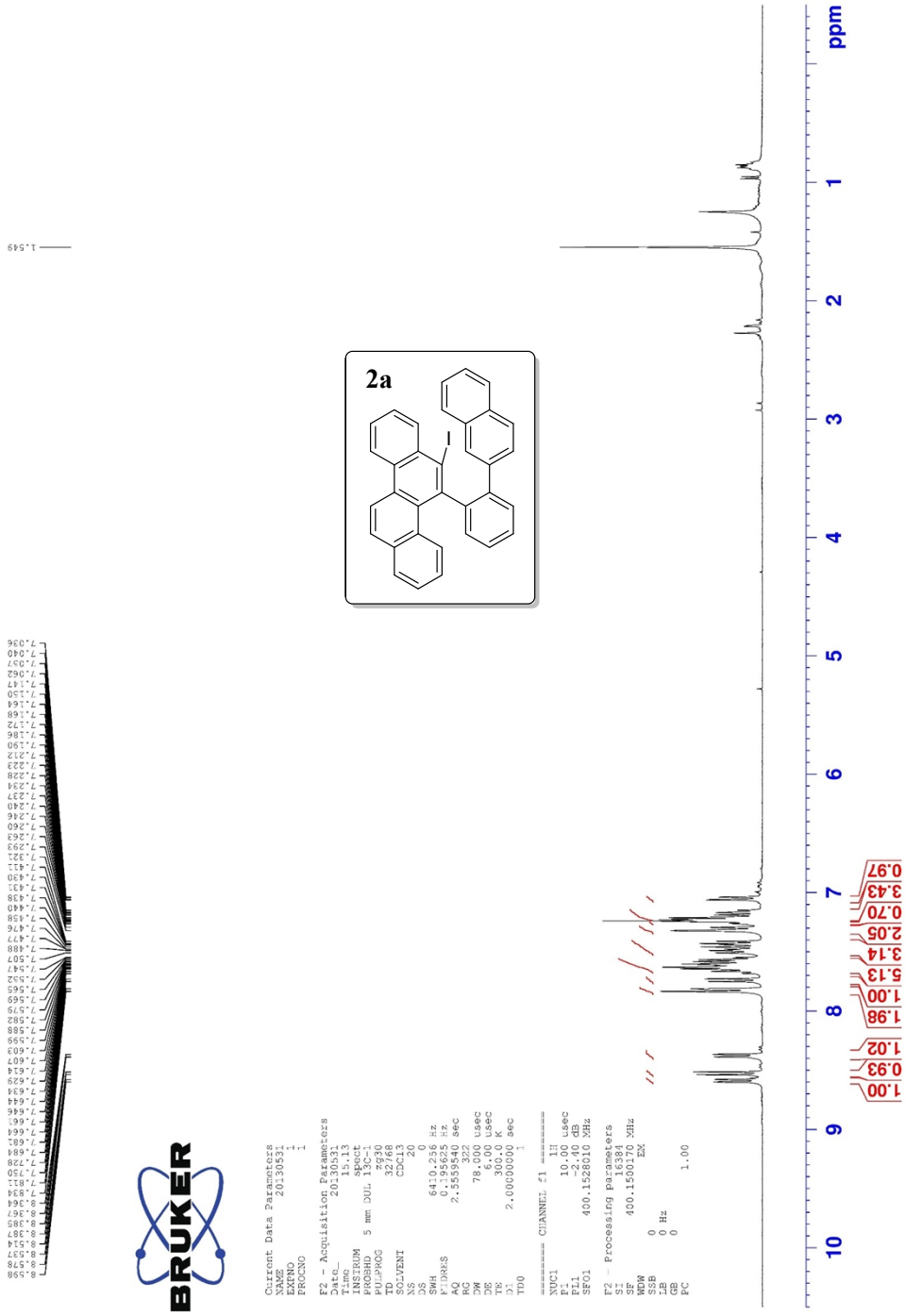

^{13}C NMR and DEPT of Compound **2a**

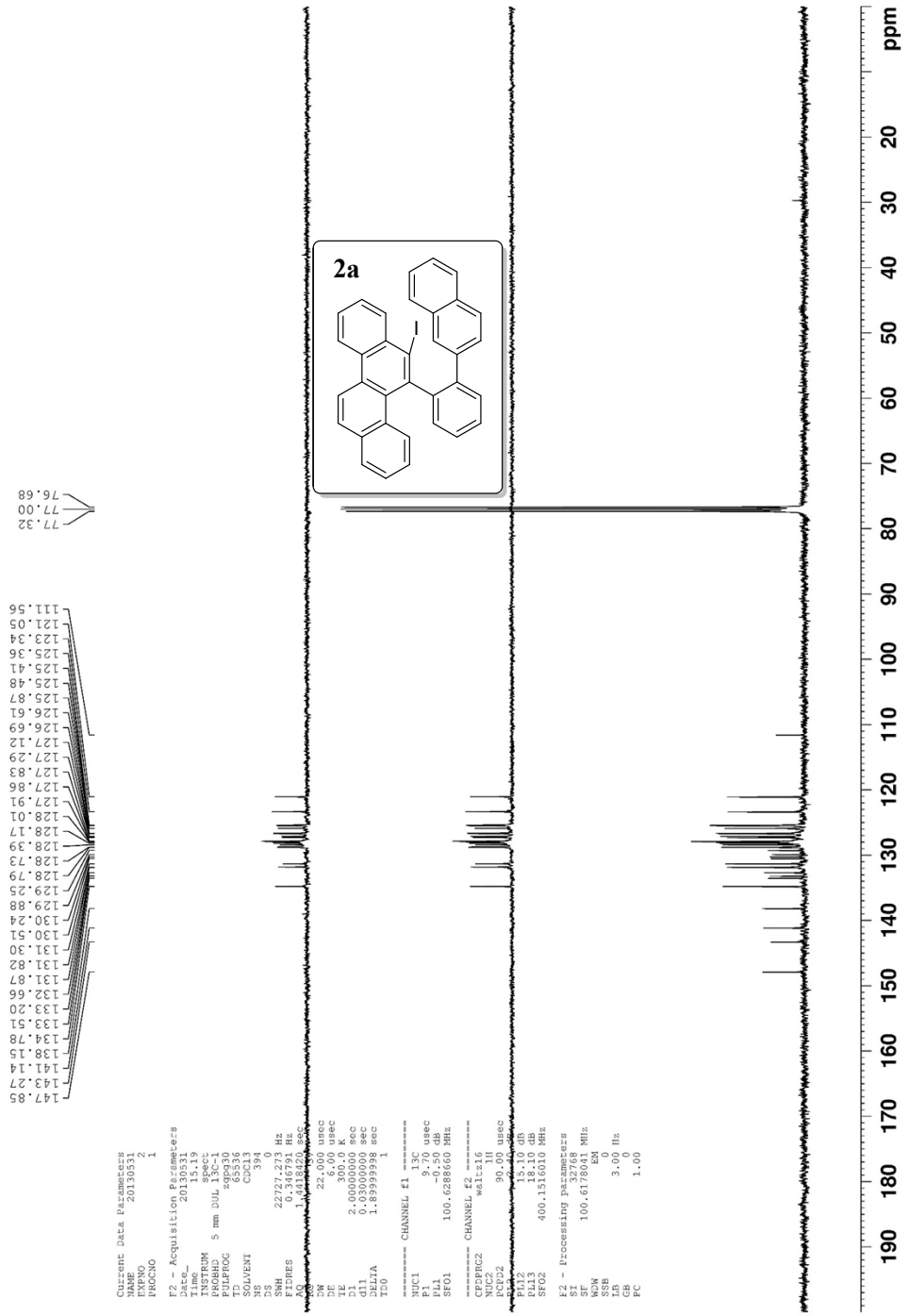

^{1}H NMR of Compound **3a**

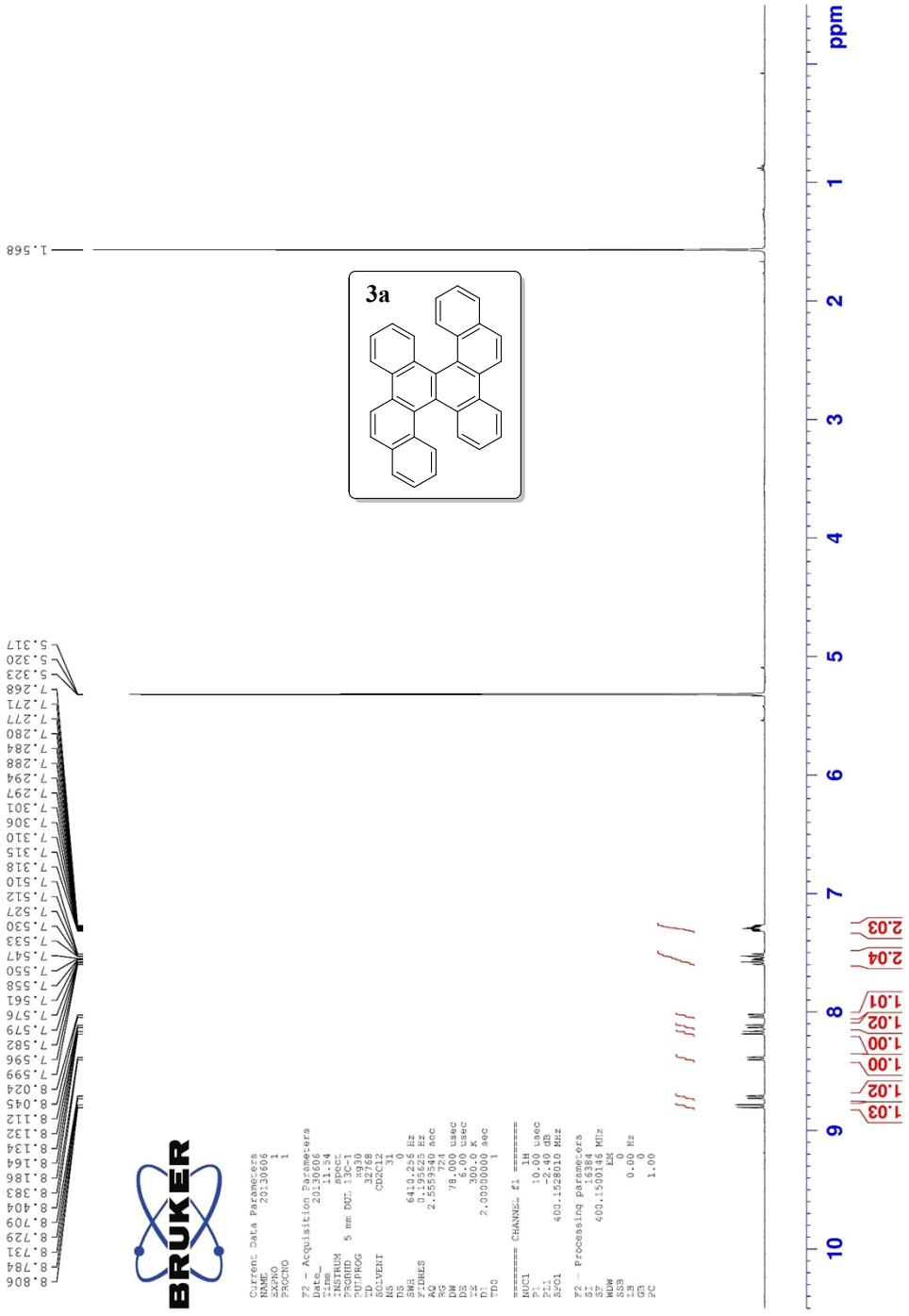

^{13}C NMR and DEPT of Compound **3a**

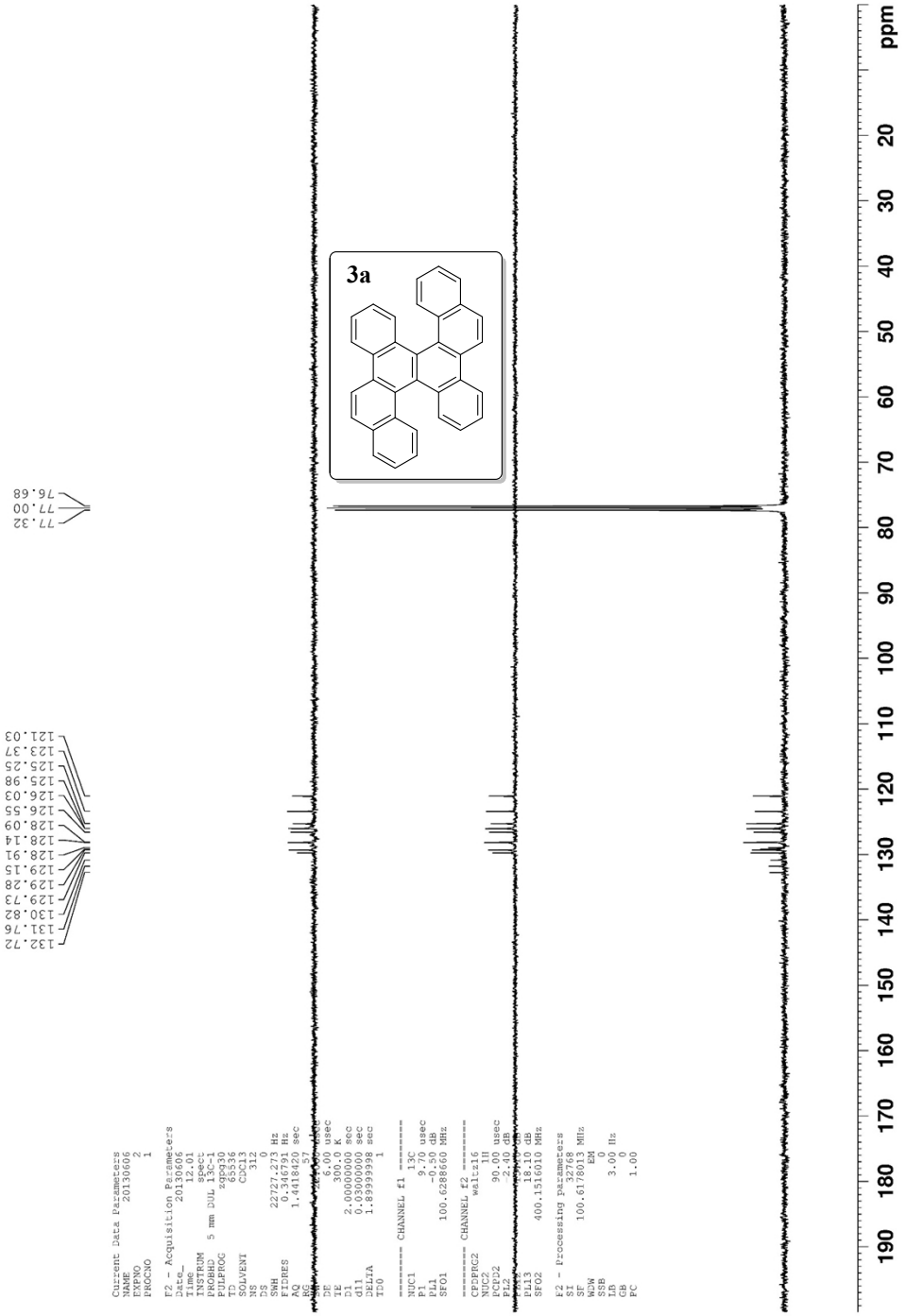

^{1}H NMR of Compound **1b**

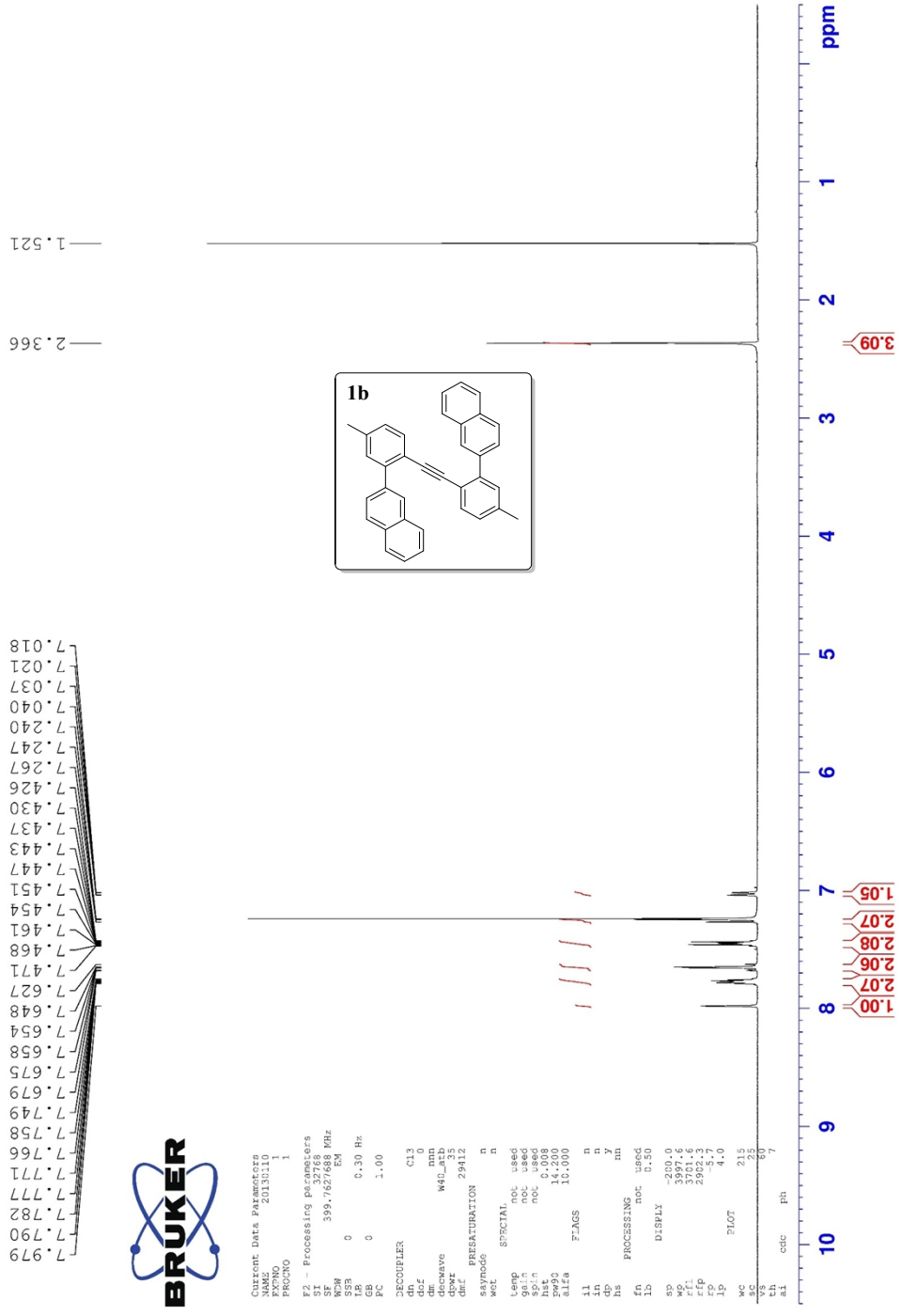

^{13}C NMR and DEPT of Compound **1b**

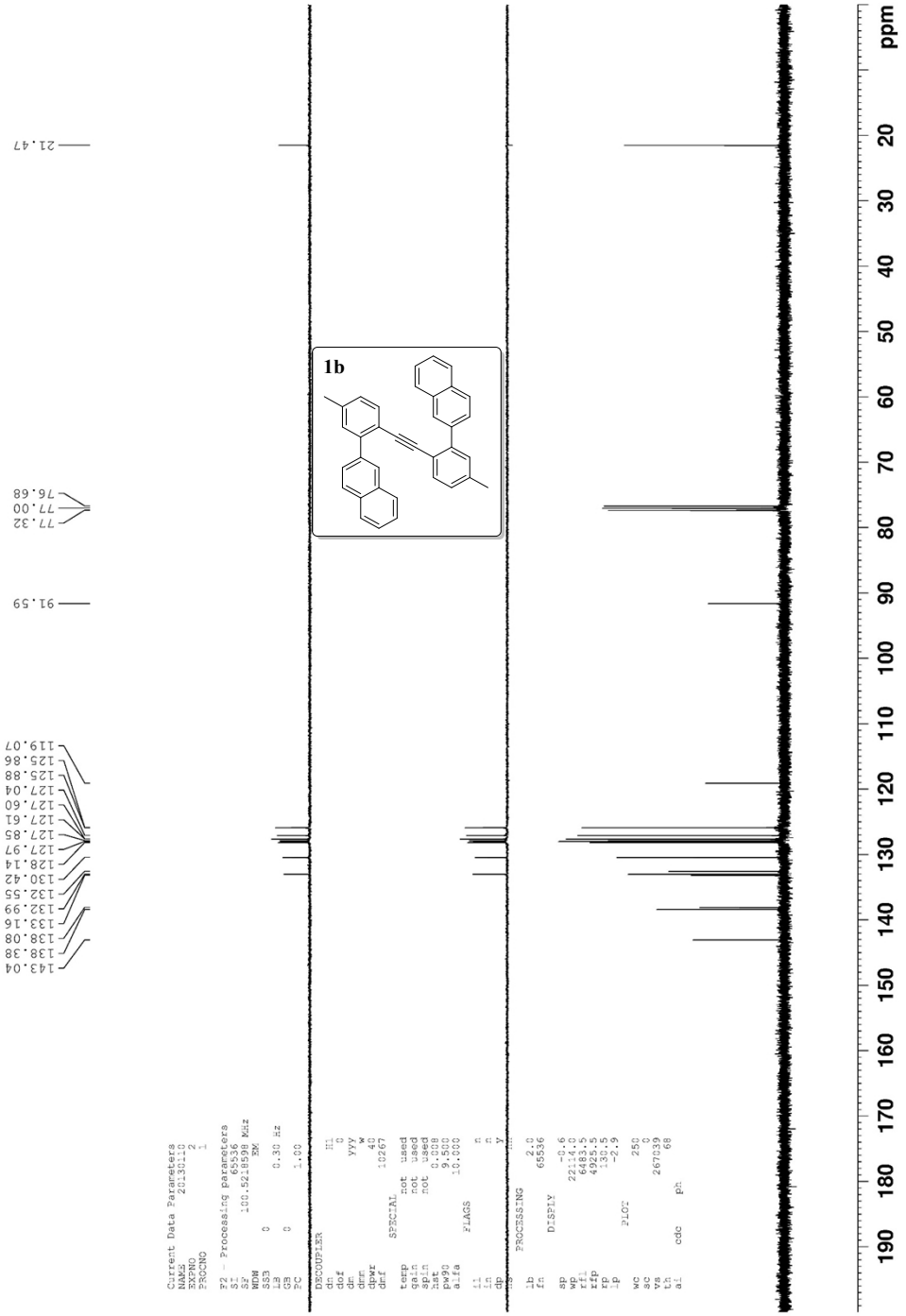

^{1}H NMR of Compound **2b**

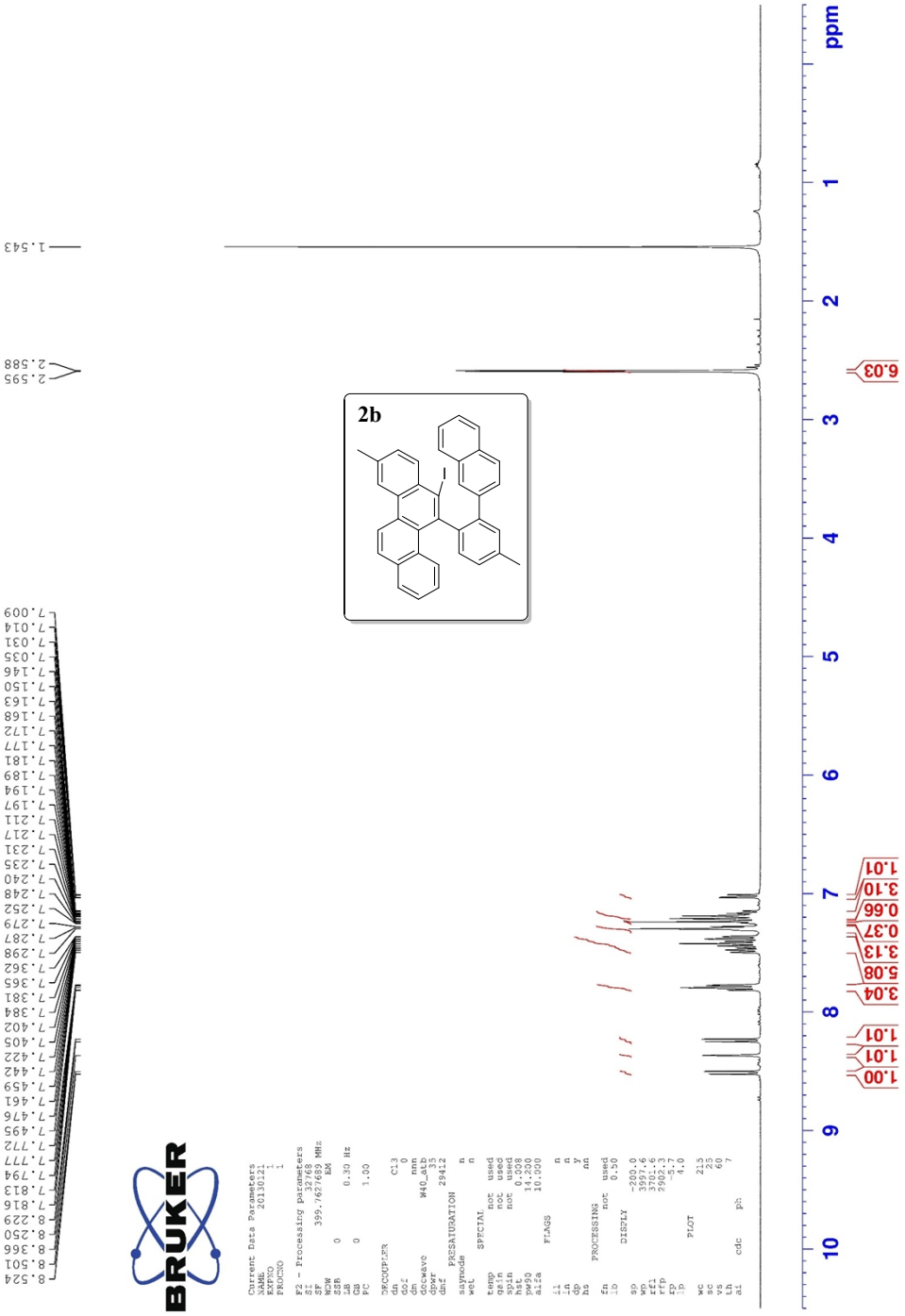

^{13}C NMR and DEPT of Compound **2b**

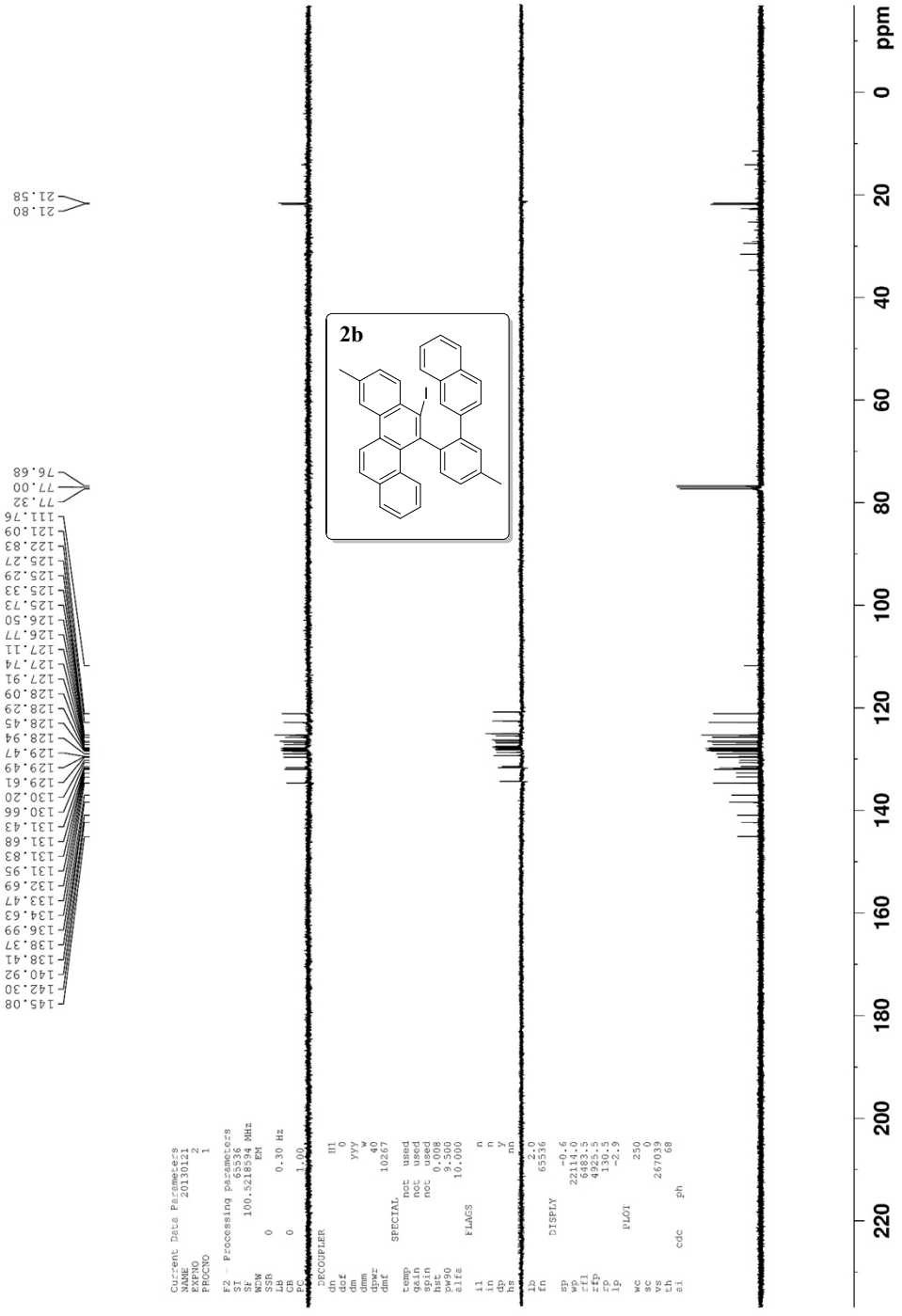

^{1}H NMR of Compound **3b**

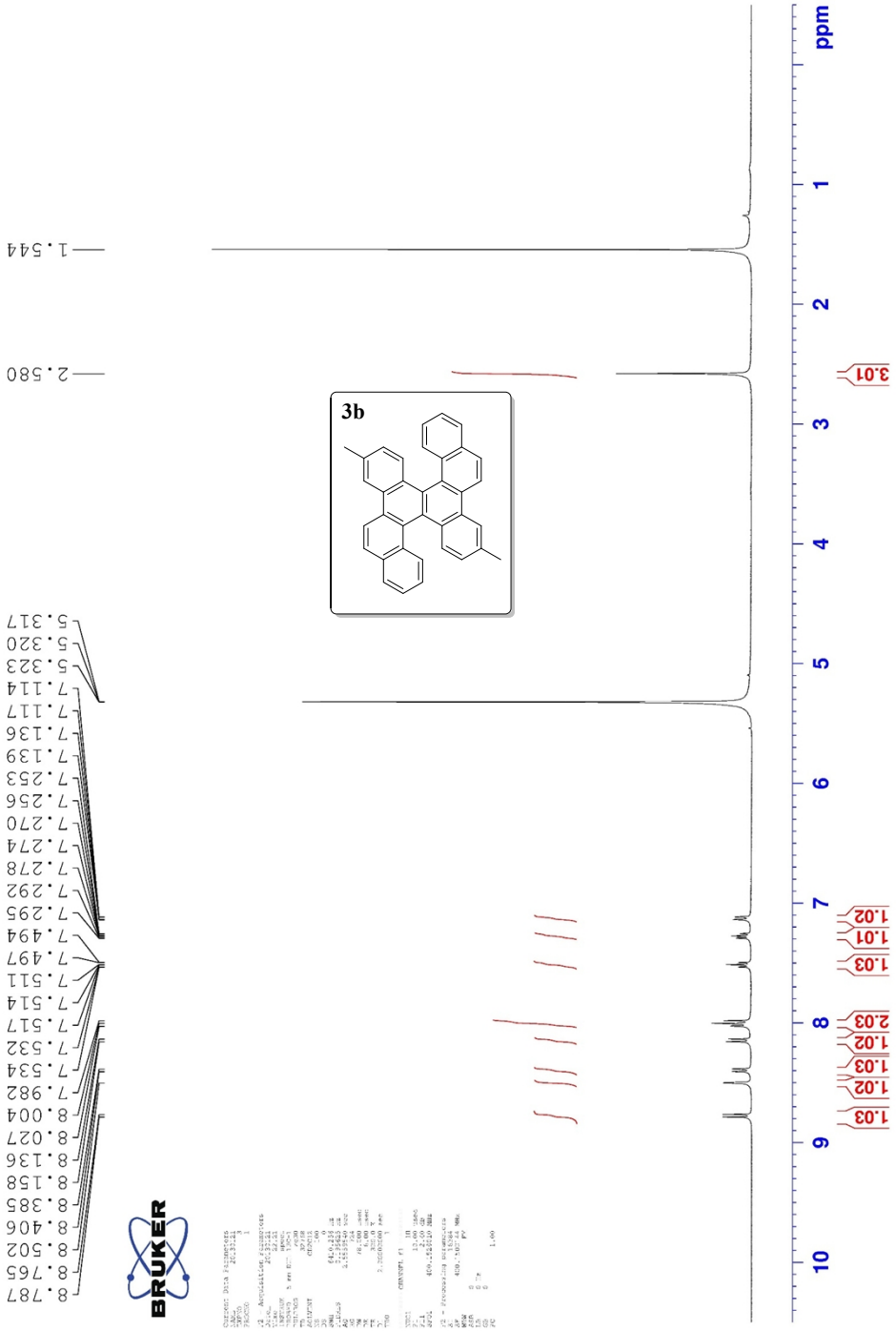

^{13}C NMR and DEPT of Compound **3b**

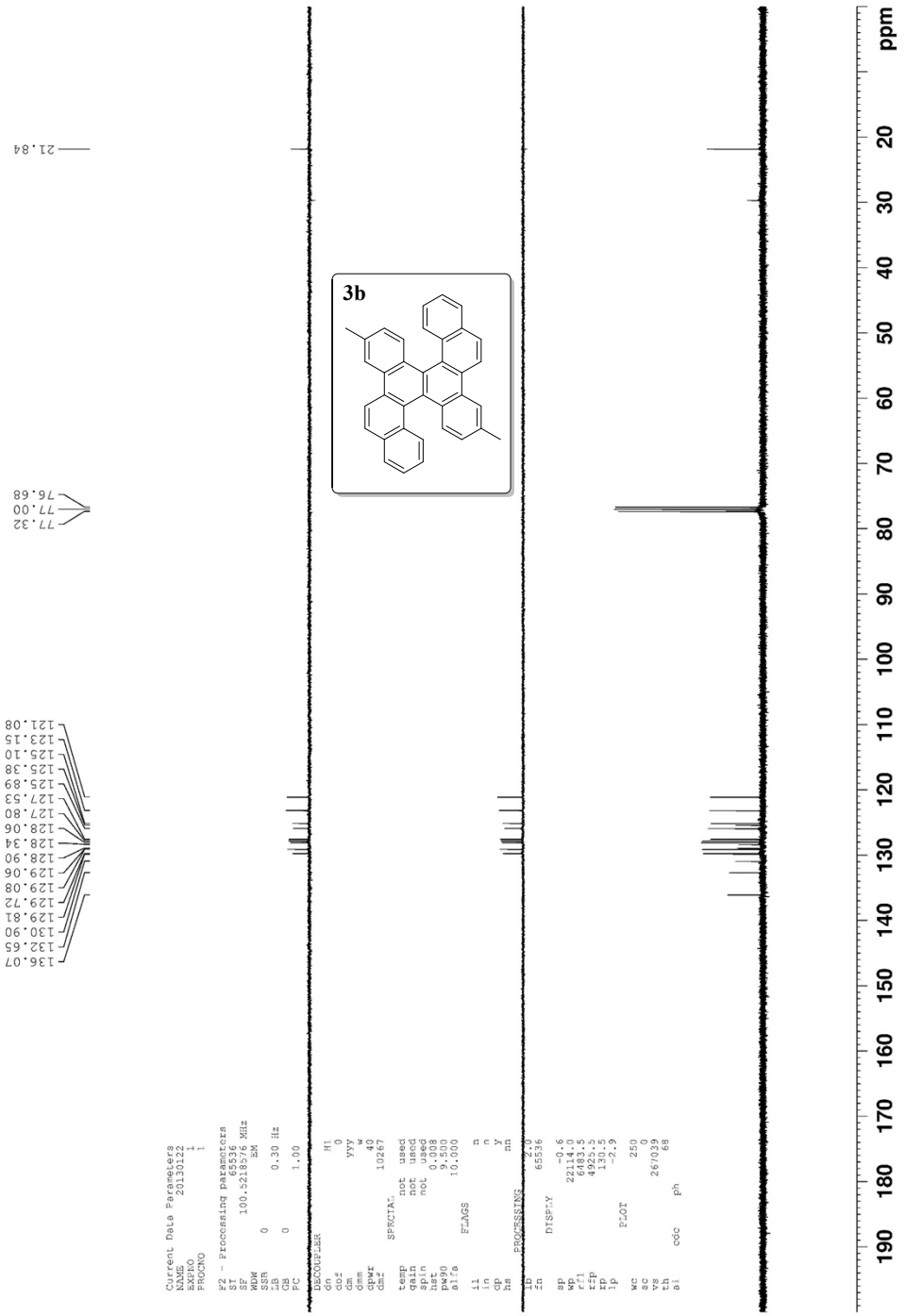

^{1}H NMR of Compound **1c**

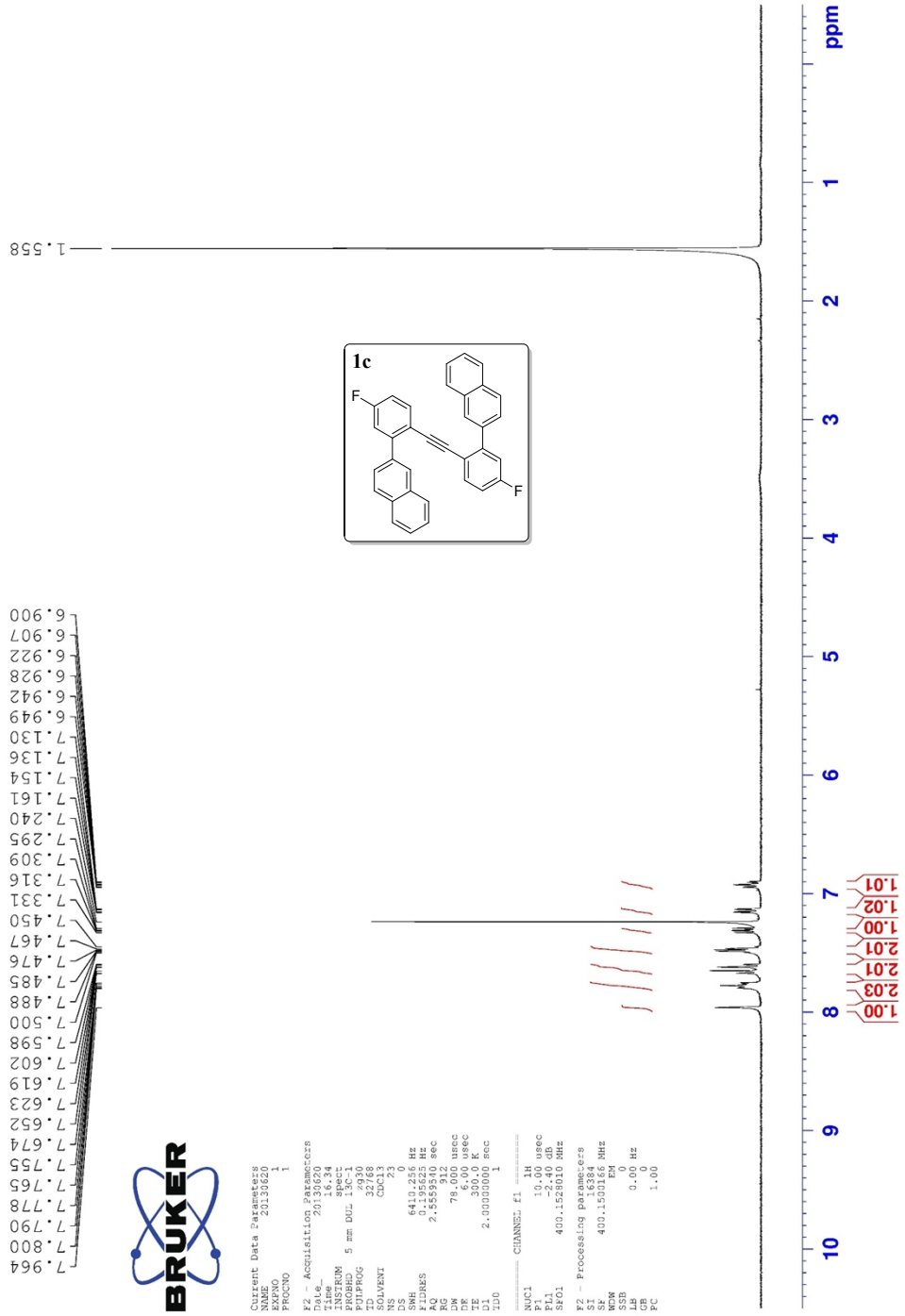

^{13}C NMR and DEPT of Compound **1c**

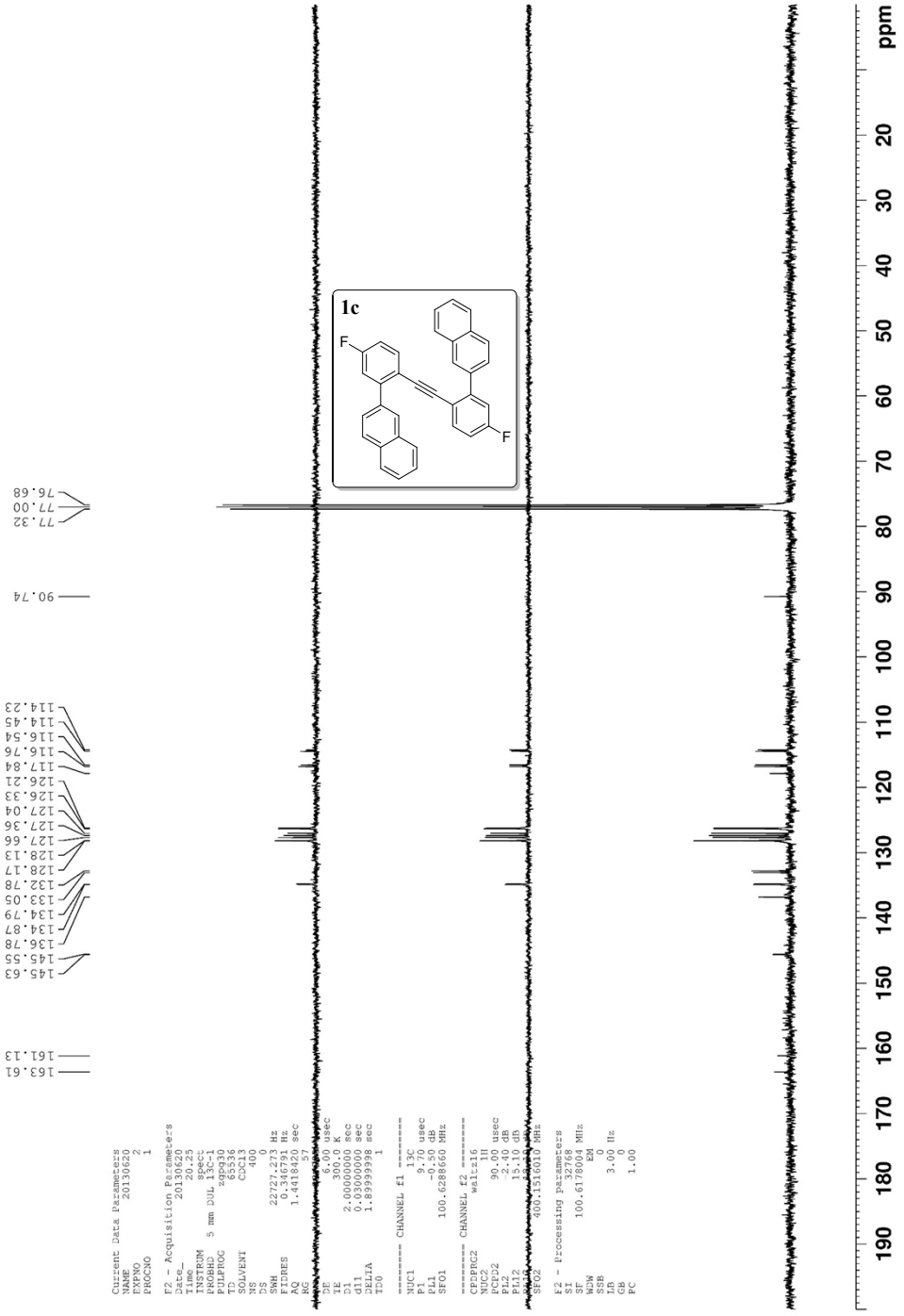

^{1}H NMR of Compound **2c**

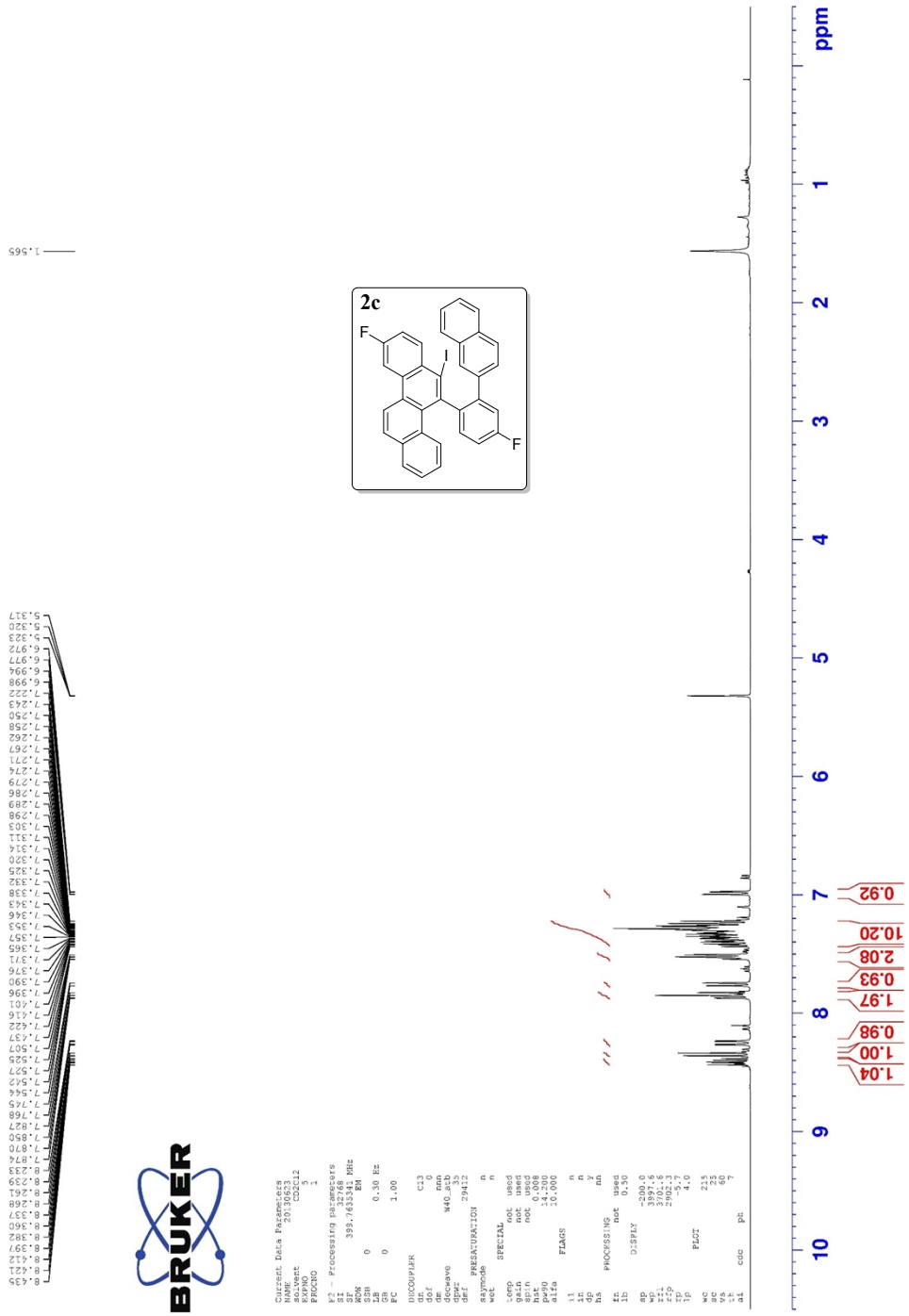

^{13}C NMR and DEPT of Compound **2c**

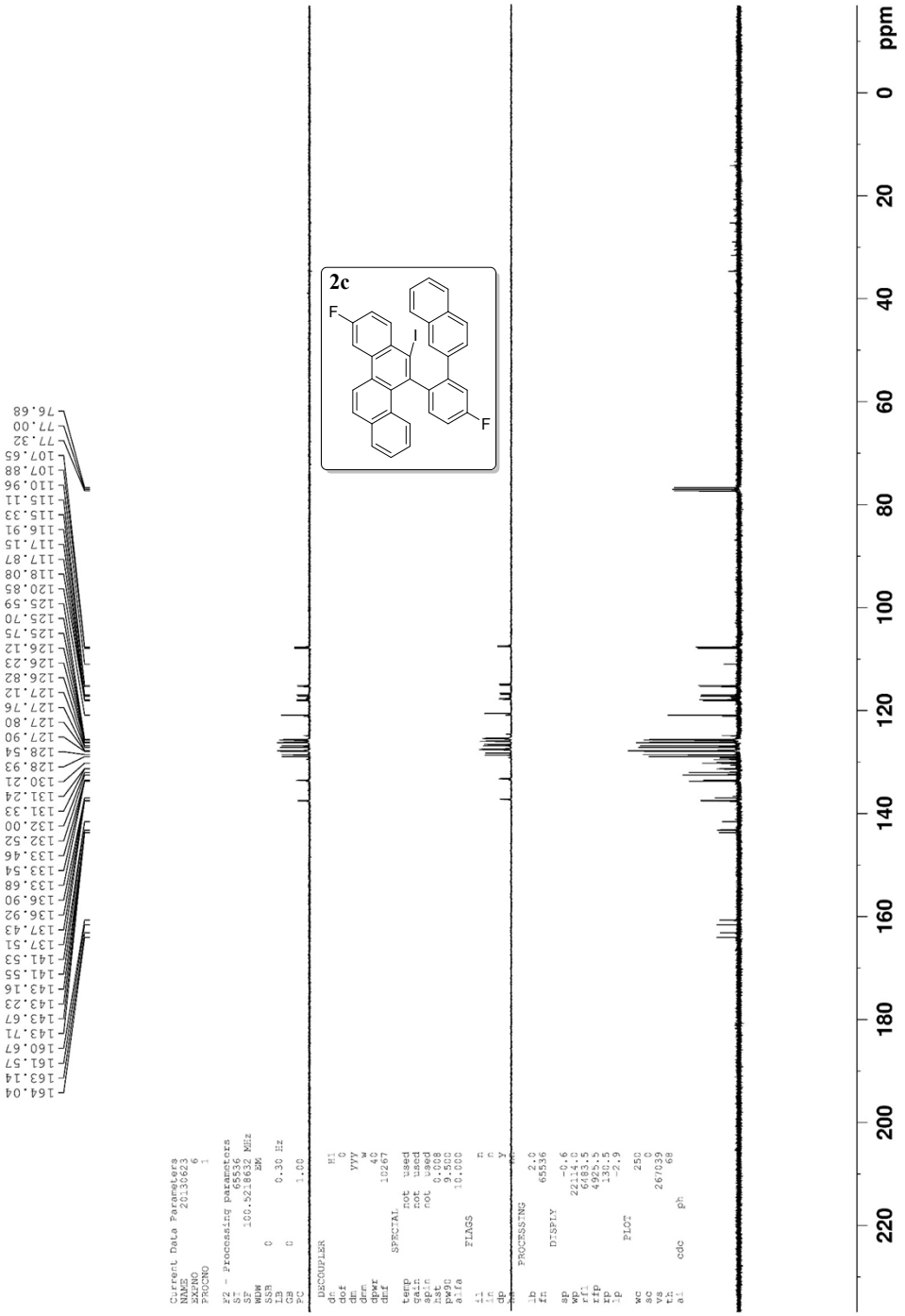

^{1}H NMR of Compound **3c**

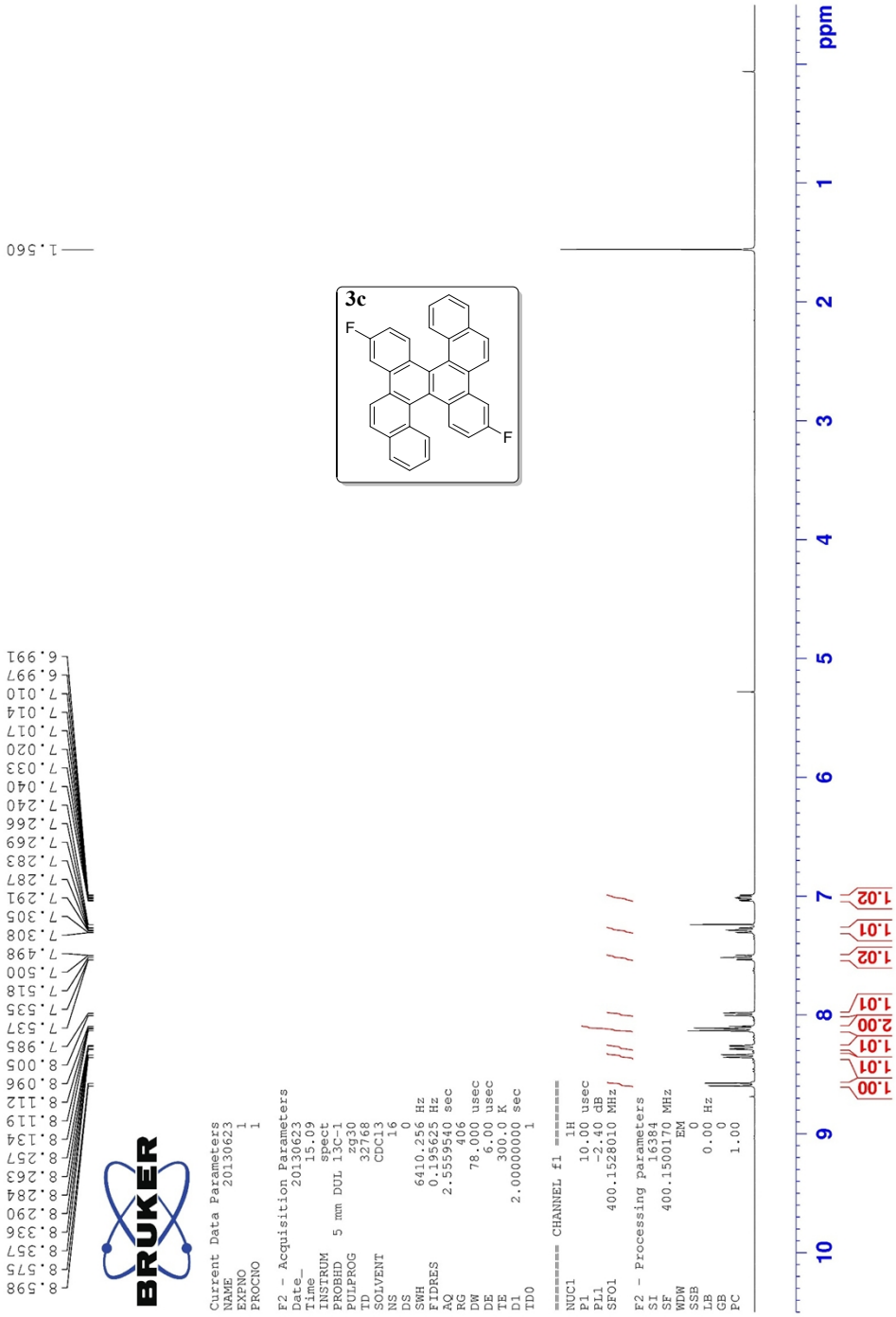

^{13}C NMR and DEPT of Compound **3c**

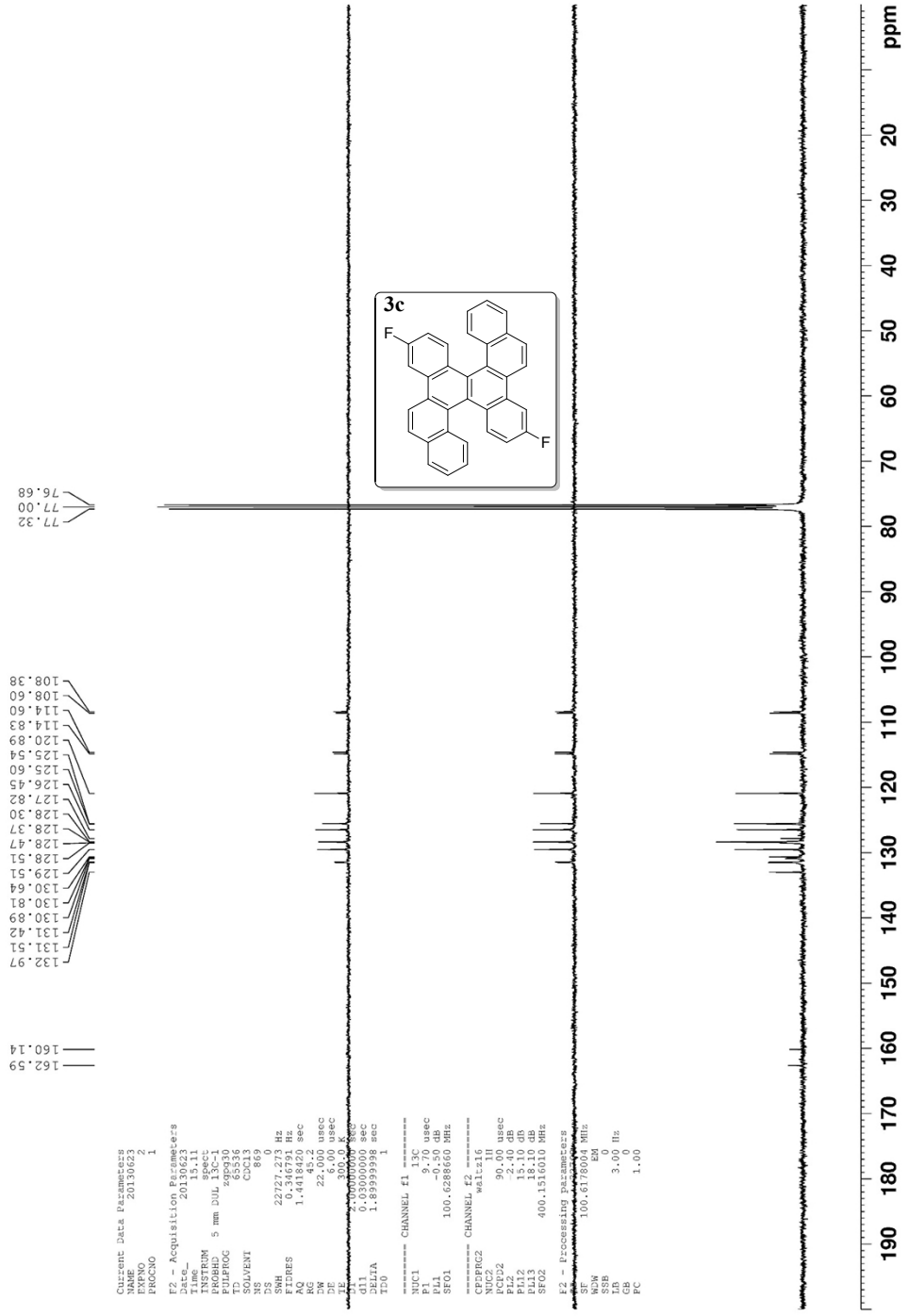

^{1}H NMR of Compound **1d**

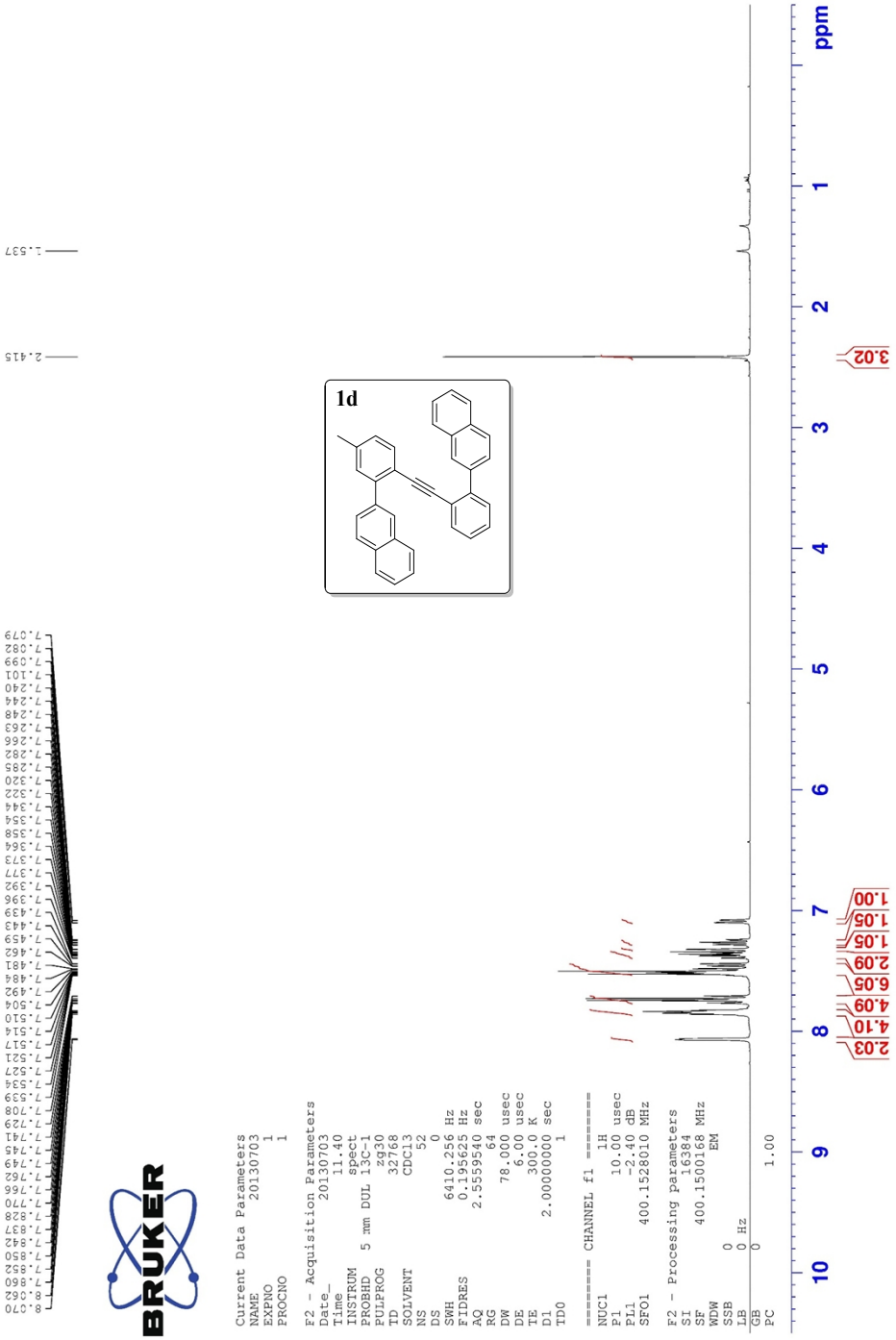

^{13}C NMR and DEPT of Compound **1d**

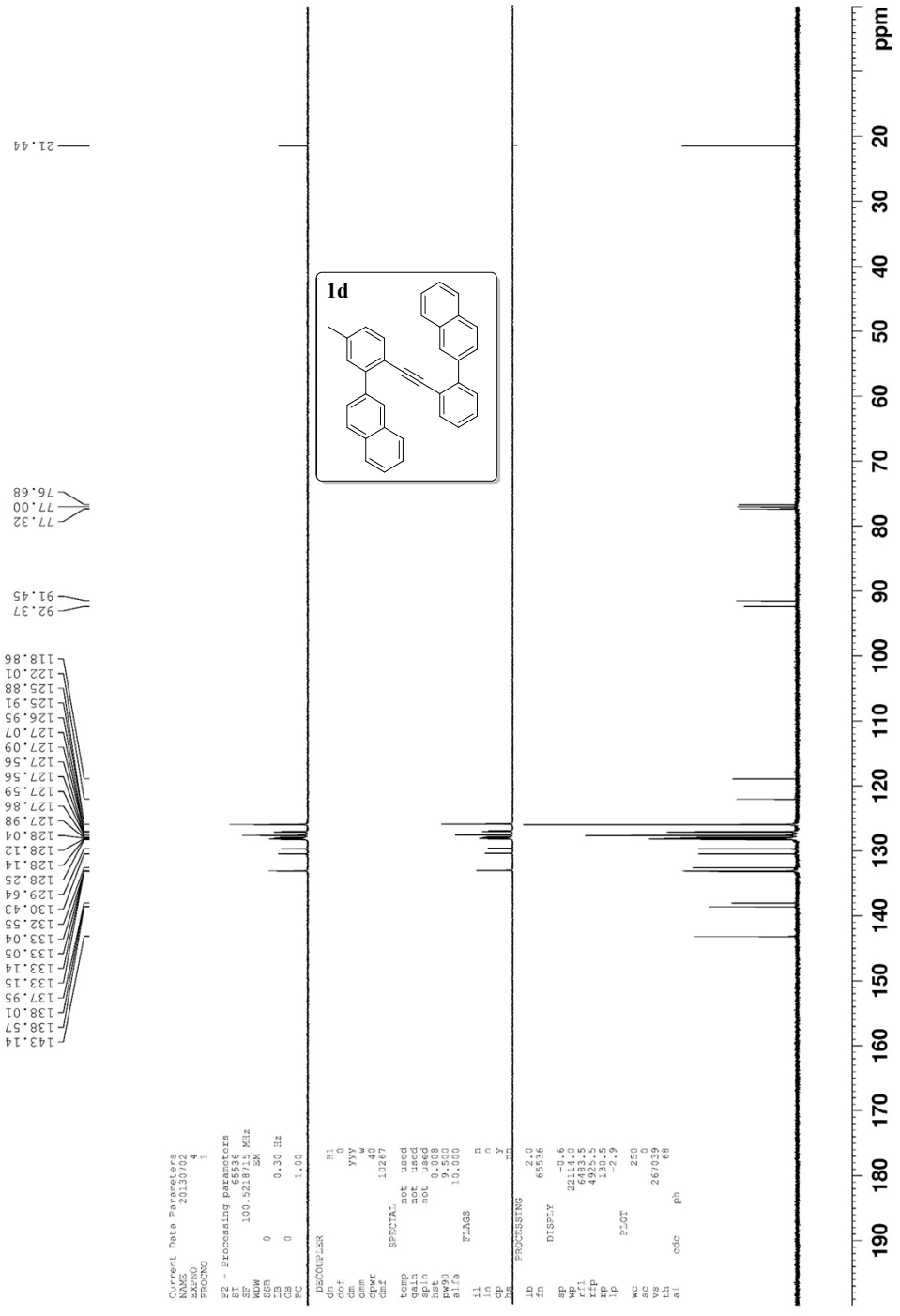

^{1}H NMR of Compound **3d**

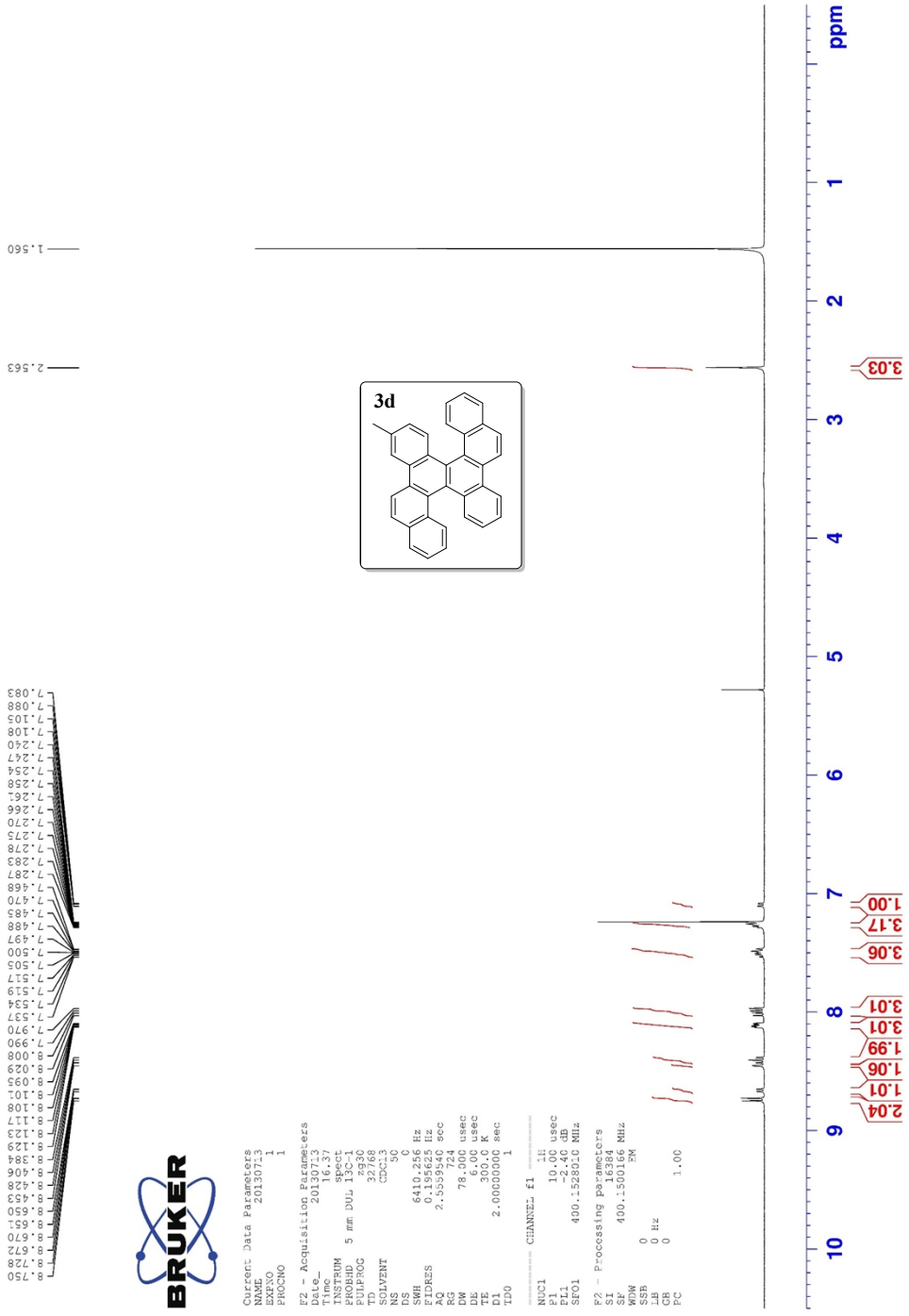

^{13}C NMR and DEPT of Compound **3d**

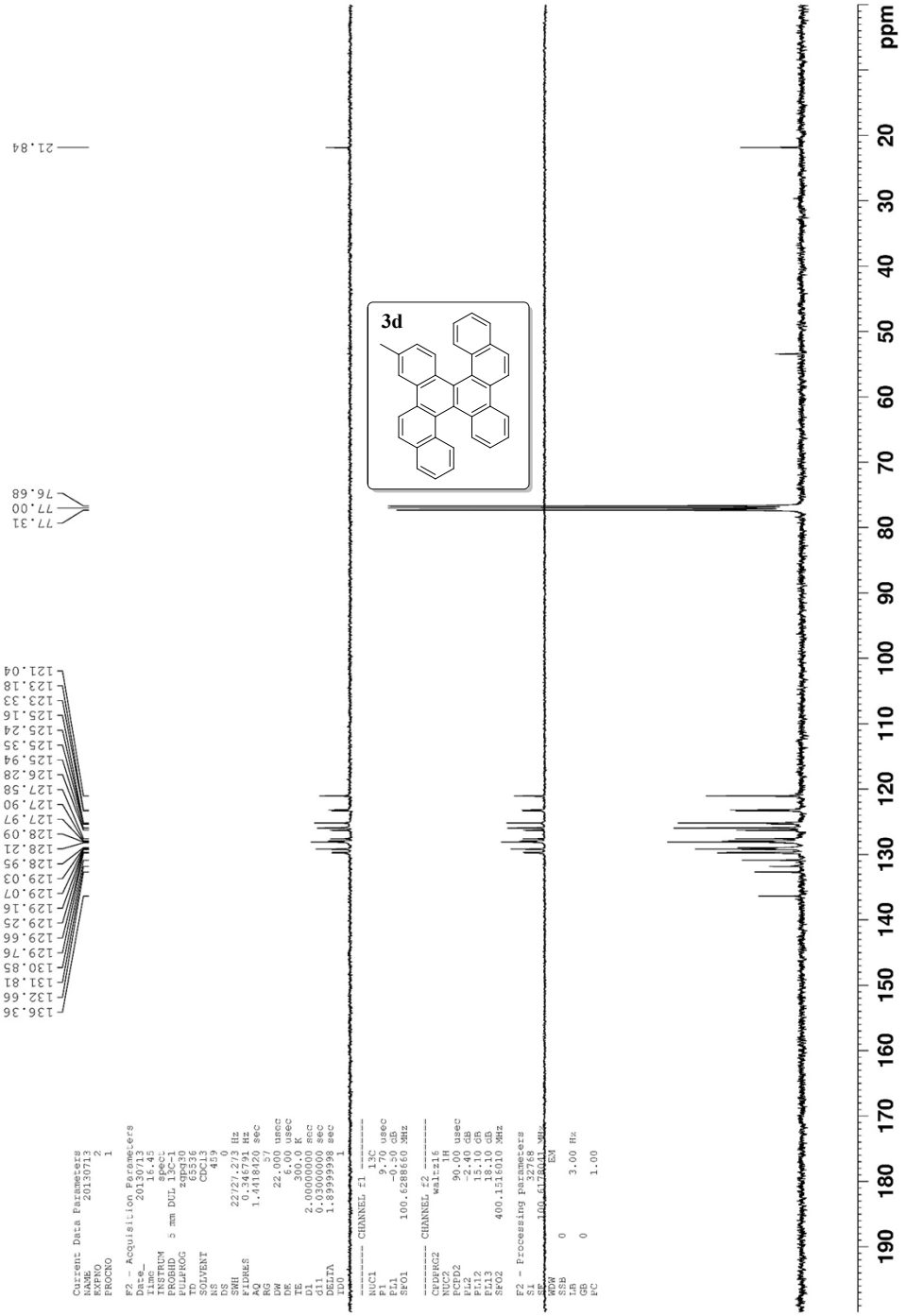

(E) HRMS mass spectra for key compounds **4a-4d**

HRMS of Compound **4a**

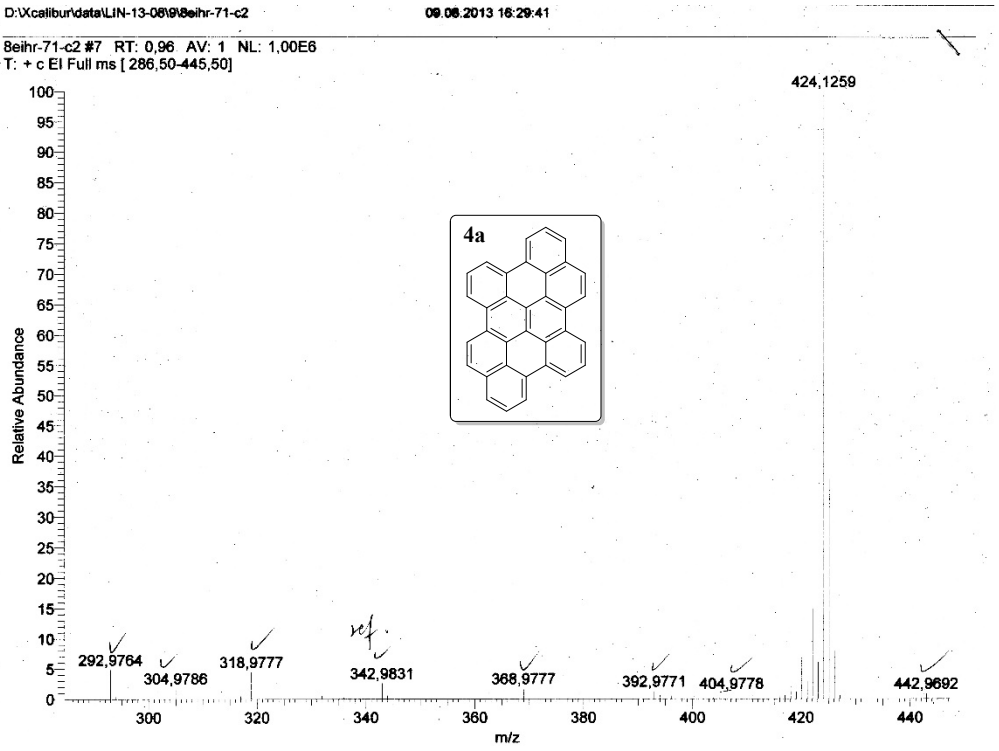

HRMS of Compound **4b**

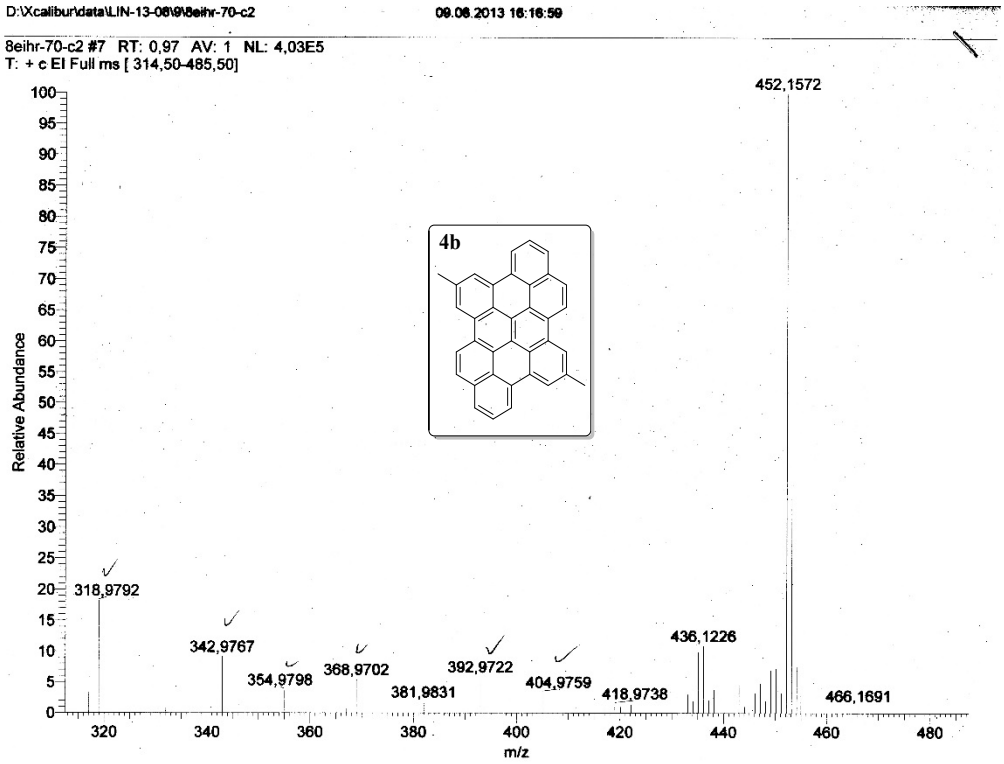

HRMS of Compound **4c**

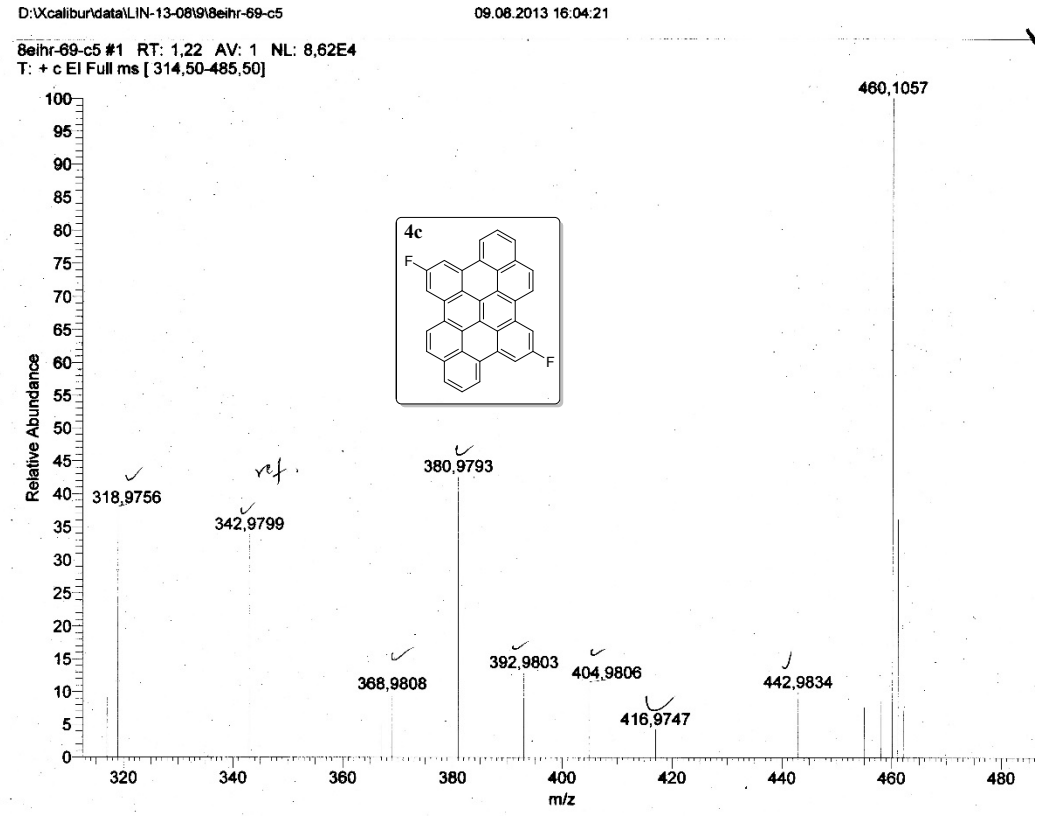

HRMS of Compound **4d**

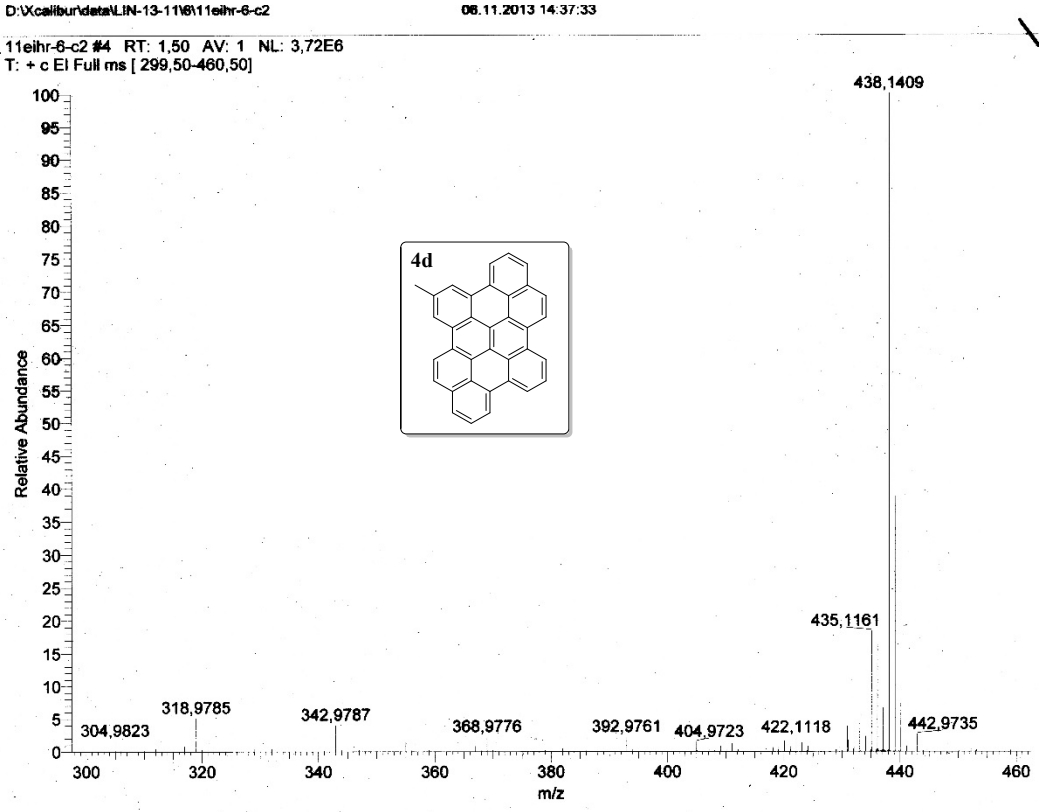

(F) Computational details

Density functional theory computation was used for determining the structures and the energies of molecules **4a**–**4e**. The neutral and cationic calculations are with the (U)B3LYP functional and 6-31G* basis set.[1] The inner reorganization energy (λ_{in}) is calculated with the four-point method: [2]

$$\lambda_{in} = \left(E(N,C_{opt}) - E(N,N_{opt})\right) + \left(E(C,N_{opt}) - E(C,C_{opt})\right),$$

where $E(A,B)$ is the energy obtained form state A at coordinate B, and $N_{opt}(C_{opt})$ is the optimized structure of the neutral (cationic) molecule. The calculating results were listed in **Table SF1**. The outer reorganization energy (λ_{out}) is set as 30 meV for aromatic molecules in a nonpolar environment. The total reorganization (λ) is the sum of λ_{in} and λ_{out}.

Table SF1. Calculating inner reorganization energy (λ_{in}) by B3LYP/6-31G*.

Compound	**4a**	**4b**	**4c**	**4d**	**4e**
λ_{in} (meV)	100.0	126.3	117.3	100.4	103.7

The electronic coupling (V) for the charge hopping process was evaluated by the direct coupling (DC) scheme.[3] The electronic coupling values were calculated by the LC-ωPBE[4] scheme (ω = 0.2) and the Dunning's double-ζ basis sets (DZP)[5]. In DC calculations, we first obtained two charge-localized states for the reactant state Ψ_r and the product state Ψ_p. The electronic coupling was then evaluated by

$$V = \frac{H_{rp} - (E_r + E_p)/2}{1 - S_{rp}^2},$$

where E_r and E_p are the energies for the reactant state and the product state, and H_{rp} and S_{rp} are the off-diagonal matrix elements for the Hamiltonian and the overlap matrix, respectively. All the quantum chemistry calculations were performed with a developmental version of Q-Chem.[6]

The dimer configurations for the electronic coupling calculation were obtained from the crystals. The calculated values are listed in **Table SF2**. To see the thermal fluctuation of the electronic coupling, we also sample the configurations from molecular dynamics (**MD**) simulations in the canonical ensemble (**NVT**) at 298 K. The **MD** simulation was performed using the Tinker program with the MM3 force field.[7] The supercell was formed with 64 molecules arranged in a $4 \times 4 \times 4$ array

(**Figure SF1**), following the crystal structure. The simulation time step is 1 fs. The trajectories were recorded with time interval of 1 ps. We sampled the dimer configurations with neighbors of a central molecule after equilibrating the system for 100 ps. The distributions of coupling strengths, together with our multi-Gaussian fitting, are shown in Figures SF2-SF5.

Table SF2. Calculated electronic coupling of hopping pathway in crystal

Compound	Pathway	Length r_i (Å)	Character	V (meV)
4a	I	5.133	π-π	0.21
4a	II	8.1846	herringbone	29.51
4a	III	11.5659	inter-layer	13.22
4a	IV	12.6538	inter-layer	0.66
4a	V	14.1759	inter-layer	2.26
4b	I	5.0661	π-π	14.88
4b	II	8.3667	herringbone	22.72
4b	III	13.0414	inter-layer	0.11
4c	I	5.0807	π-π	11.0
4c	II	8.1912	herringbone	32.2
4c	III	11.8364	inter-layer	5.1
4c	IV	12.8808	inter-layer	0.14
4c	V	14.3398	inter-layer	2.0
4e	I	6.1038	π-π	42.0
4e	II	10.1292	inter-layer	5.9
4e	III	12.0623	inter-layer	1.4
4e	IV	13.3084	inter-layer	0.3
4e	V	13.5187	inter-layer	0.03

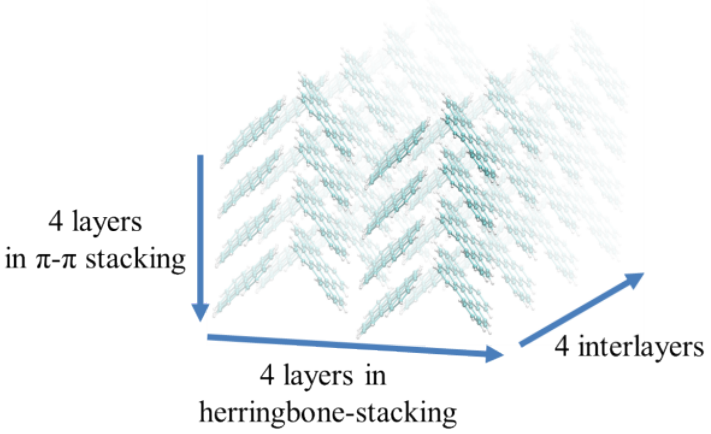

Figure SF1. The supercell of **DBBT** (**4a**) used in MD simulation.

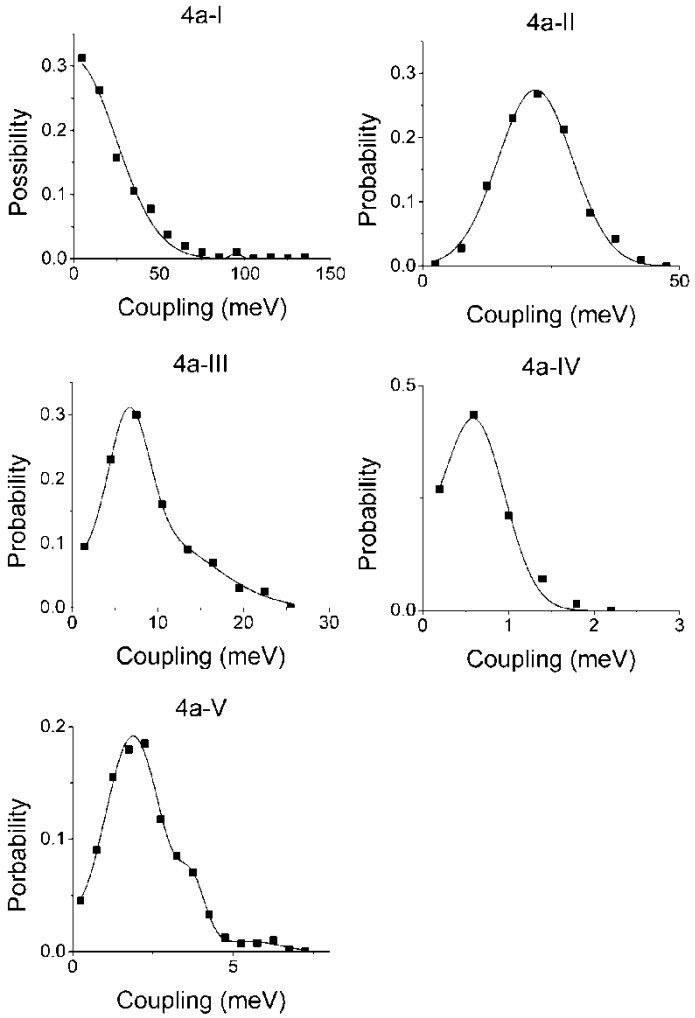

Figure SF2. Distributions of the couplings based on dimer configurations collected from MD simulation. Shown are for **4a** with its 5 different neighboring configurations.

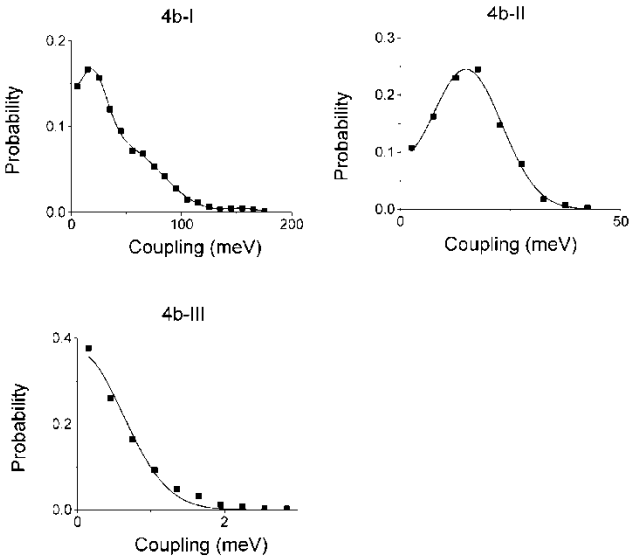

Figure SF3. Distributions of the couplings based on dimer configurations collected from MD simulation. Shown are for **4b** with its 3 different neighboring configurations.

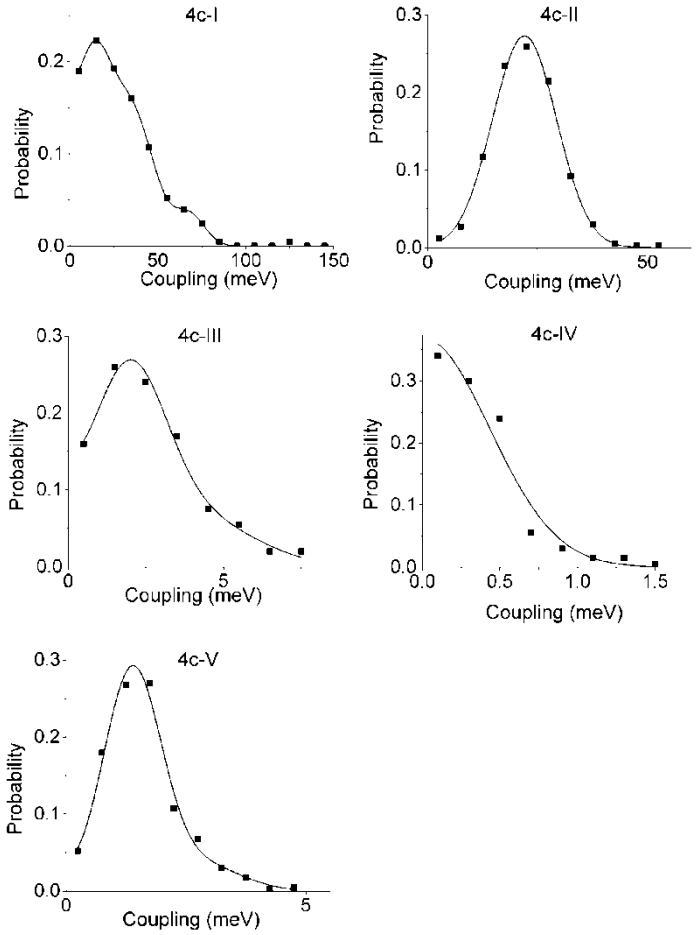

Figure SF4. Distributions of the couplings based on dimer configurations collected

from MD simulation. Shown are for **4c** with its 5 different neighboring configurations.

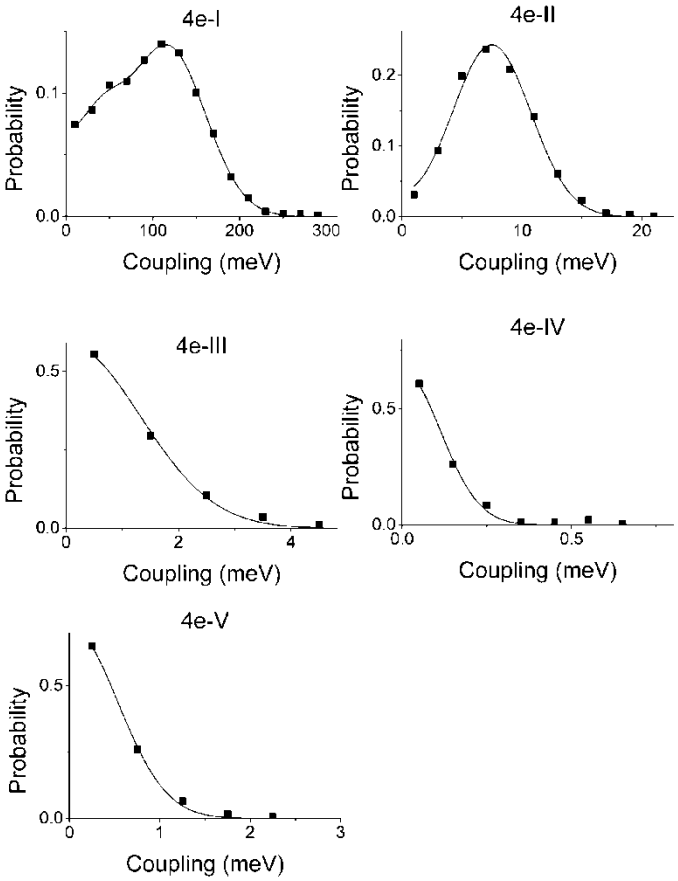

Figure SF5. Distributions of the couplings based on dimer configurations collected from MD simulation. Shown are for **4e** with its 5 different neighboring configurations.

Based on the Einstein relation, the charge mobility (μ_E) can be estimated from the diffusion coefficient:[8]

$$\mu_E = \frac{e}{k_B T} D,$$

where e is the electronic charge, k_B is the Boltzmann constant, T is temperatue and D is the diffusion coefficient. The diffusion coefficient can be calculated as

$$D \approx \frac{1}{2n} \sum_i r_i^2 k_i P_i ,$$

where n is the spatial dimensionality (n=3 in this calculation), r_i is the projection of the hopping pathway on the direction of electric field for pathway i, k_i is the hopping

rate and P_i is the hopping probability, which is proportional to the hopping rate:

$$P_i = \frac{k_i}{\sum_i k_i},$$

and the k_i can be evaluated by Marcus equation:

$$k_i = \frac{V^2}{\hbar}\sqrt{\frac{\pi}{4\lambda k_B T}}\exp\left[\frac{-\lambda}{4k_B T}\right],$$

where λ is the total reorganization of the compound. The μ_E reported in the maintext were calculated with fixed coupling values derived from crystal structure.

Kinetic Monte Carlo (KMC) simulation was carried out on the lattice of 9600 molecules under the periodic boundary condition.[9] The number of unit cells in axis, for different molecules, are included in **Table SF3**. The charge mobility is calculated by

$$\mu_{KMC} = \frac{\vec{d}}{t \cdot \vec{E}},$$

where $\vec{d}$ is the drift distance of charge carrier after one million hopping steps, *t* is the total drift time and $\vec{E}$ is the applied electric field, which is 10^5 V/cm in the simulation. The hopping time for each step is calculated as

$$t_s = \frac{r}{\sum_i k_i},$$

where k_i is the rate for the hopping process to the neighbor site *i* and the *r* is a random number following an exponential distribution $\exp(-r)$. The total drift time *t* is the sum of all t_s. For charge at each site, there are several possible hopping paths. The probability for each hopping path is proportional to their corresponding hopping rates

$$P_i = \frac{k_i}{\sum_i k_i},$$

where the inter-site hopping rate is calculated by the Marcus theory:

$$k_i = \frac{V^2}{\hbar}\sqrt{\frac{\pi}{4\lambda k_B T}}\exp\left[\frac{-(\Delta G + \lambda)^2}{4\lambda k_B T}\right].$$

The electronic coupling (V) is randomly generated by the coupling distributions obtained *via* the MD simulations, as shown by **Figure SF2** to **Figure SF5**. The Free energy ΔG is calculated by

$$\Delta G = q\vec{r_i} \cdot \vec{E} + \Delta\varepsilon,$$

where *q* is charge, $\vec{r_i}$ is the vector of hopping pathway, $\vec{E}$ is the electric field, and Δε

is energy change from the site energy ($\varepsilon_f - \varepsilon_i$). The site energies ε_i and ε_f are randomly determined with a normal distribution ρ(ε) with standard derivation of 1 k_BT,

$$\rho(\varepsilon) = \frac{1}{\sqrt{2\pi\sigma^2}}\exp\left[-\frac{\varepsilon^2}{2\sigma^2}\right]$$

Table SF3. Lattice setting

Lattice Parameter [a]	**4a**	**4b**	**4c**	**4e**
a	11.5659	5.0661	11.8364	26.659
b	5.13300	15.948	5.0807	6.1038
c	15.5436	25.586	15.5746	19.317
α	90	90	90	90
β	90.06	90	90.49	95.08
γ	90	90	90	90
Number of unit cells employed in simulation				
N_a x N_b x N_c	8 x 100 x 6	100 x 6 x 4	8 x 100 x 6	4 x 100 x 6

[a] in the units of angstroms (a, b and c) and degrees (α, β, and γ).

When the intersite coupling is larger than the reorganization energy by one k_BT, we assume the charge is delocalized among these sites, forming a charge delocalized domain *D*. Therefore, we employed a delocalized model for the polaron.[10] The delocalized state (ψ_i) is obtained by the linear recombination of the localized state ($|a\rangle$)

$$|\psi_i\rangle = \sum_{a \in D} c_{ia}|a\rangle ,$$

which is the eigenstate of the Hamiltonian for the delocalized polaron:

$$H = \sum_{a \in D} \varepsilon_a |a\rangle\langle a| + \sum_{a,b \in D, a>b} (V_{ab}|a\rangle\langle b| + h.c.) ,$$

and the corresponding eigenvalue is ε_i. In the Hamiltonian, *h.c.* stands for Hermition conjugate. In simulation, the diagonal single-site energies ε_a was sampled from a normal distribution with standard derivation of 1 k_BT, and the coupling V_{ab} was sampled with the distribution obtained from MD simulation.

The hopping rate between the delocalized states ψ_i and ψ_f is

$$k_{if} = \frac{2\pi}{\hbar}|V_{if}|^2 \frac{1}{\sqrt{4\pi\lambda_{if}k_BT}} exp\left[-\frac{(\lambda_{if}+\Delta G_{if})^2}{4\lambda_{if}k_BT}\right].$$

The electronic coupling V_{if} is

$$V_{if} = \langle\psi_i | H | \psi_f\rangle = \sum_a \sum_b c_{ia}c_{fb}V_{ab} ,$$

where the V_{ab} is the intersite coupling between site a and site b
$V_{ab} = \langle a | H | b\rangle$.

The change of free energy ΔG_{if} is

$$\Delta G_{if} = q\vec{r}_{if} \cdot \vec{E} + \varepsilon_f - \varepsilon_i ,$$

where the ε_i (ε_f) are the eigenenergy of delocalized state i (f), $\vec{r}_{if}$ is the hopping distance given by

$$\vec{r}_{if} = \vec{r}_f - \vec{r}_i ,$$

where the $\vec{r}_j$ is the location of the state ψ_j, estimated by an weighted averaged value with the probability of the charge at the site $|c_{ja}|^2$ as the weighting factor:

$$r_j = \sum_{a \in D} |c_{ja}|^2 r_a .$$

The reorganization energy λ for the delocalized polaron is given by an averaged value of the initial and final state, with each λ calculated from as a weighted average of each molecule, with $|c_{ia}|^4$ as the weighting factor which accounts for the participation ratio.[10]

$$\lambda_{if} = \frac{1}{2}(\lambda_i + \lambda_f) = \frac{\lambda}{2}\left[\sum_{a \in D_i} |c_{ia}|^4 + \sum_{b \in D_f} |c_{fb}|^4\right] ,$$

where D_i and D_f are the domains for the initial and final states, or the range of the donor and acceptor polarons, respectively. The site energy ε_a and coupling V_{ab} were randomly generated. In our work we have generated 100 such disorder Hamiltonians. The charge mobility (μ_{KMC}) was evaluated by an averaged value of one thousand simulating results, with 10 trajectories obtained from each of the 100 randomly generated Hamiltonians. In all the charge mobilities reported, the statistical errors are less than 1%.

Table SF4. Statistical error (%) for the averaged mobilities obtained through Monte Carlo Simulations

	4a	**4b**	**4c**	**4e**
μ_{KMC}	0.27	0.54	0.25	0.95
μ_{deloc}	0.07	0.60	0.07	0.91

Reference:

1 (a) A. D. Becke, *J. Chem. Phys.* 1993, **98**, 5648−5652. (b) C. Lee, W. Yang, R. G. Parr, *Phys. Rev. B* 1988, **37**, 785−789. (c) S. H. Vosko, L. Wilk, M. Nusair,

Can. J. Phys. 1980, **58**, 1200−1211. (d) R. E. Stratmann, G. E. Scuseria, M. J. Frisch, *J. Chem. Phys.* 1998, **109**, 8218−8224. (e) R. Bauernschmitt, R. Ahlrichs, *Chem. Phys. Lett.* 1996, **256**, 454−464. (f) M. E. Casida, C. Jamorski, K. C. Casida, D. R. Salahub, *J. Chem. Phys.* 1998, **108**, 4439−4449.

2 (a) B. C. Lin, C. P. Cheng, Z. P. M. Lao, *J. Phys. Chem. A* 2003, **107**, 5241−5251. (b) Malagoli, M.; Brédas, J. *Chem. Phys. Lett.* 2000, **327**, 13−17.

3 A. Farazdel, M. Dupuis, E. Clementi, A. Aviram, *J. Am. Chem. Soc.* 1990, **112**, 4206−4214.

4 (a) M. A. Rohrdanz, K. M. Martins, J. M. Herbert, *J. Chem. Phys.* 2009, **130**, 054112. (b) You, Z.-Q.; Hung, Y.-C.; Hsu, C.-P. *J. Phys. Chem. B,* 2015, Article ASAP.

5 T. H. Dunning, *J. Chem. Phys.* 1970, **53**, 2823−2833.

6 Y. Shao, Z. Gan, E. Epifanovsky, A. T. B. Gilbert, M. Wormit, J. Kussmann, A. W. Lange, A. Behn, J. Deng, X. Feng, D. Ghosh, M. Goldey, P. R. Horn, L. D. Jacobson, I. Kaliman, R. Z. Khaliullin, T. Kuś, A. Landau, J. Liu, E. I. Proynov, Y. M. Rhee, R. M. Richard, M. A. Rohrdanz, R. P. Steele, E. J. Sundstrom, H. L.; Zimmerman, P. M.; Zuev, D.; Albrecht, B.; Alguire, E.; Austin, B. Woodcock, G. J. O. Bera, Y. A. Bernard, E. Berquist, K. Brandhorst, K. B. Bravaya, S. T. Brown, D. Casanova, C.-M. Chang, Y. Chen, S. H. Chien, K. D. Closser, D. L. Crittenden, M. Diedenhofen, R. A. DiStasio, H. Do, A. D. Dutoi, R. G. Edgar, S. Fatehi, L. Fusti-Molnar, A. Ghysels, A. Golubeva-Zadorozhnaya, J. Gomes, M. W. D. Hanson-Heine, P. H. P. Harbach, A. W. Hauser, E. G. Hohenstein, Z. C. Holden, T.-C. Jagau, H. Ji, B. Kaduk, K. Khistyaev, J. Kim, J. Kim, R. A. King, P. Klunzinger, D. Kosenkov, T. Kowalczyk, C. M. Krauter, K. U. Lao, A. D. Laurent, K. V. Lawler, S. V. Levchenko, C. Y. Lin, F. Liu, E. Livshits, R. C. Lochan, A. Luenser, P. Manohar, S. F. Manzer, S.-P. Mao, N. Mardirossian, A. V. Marenich, S. A. Maurer, N. J. Mayhall, E. Neuscamman, C. M. Oana, R. Olivares-Amaya, D. P. O'Neill, J. A. Parkhill, T. M. Perrine, R. Peverati, A. Prociuk, D. R. Rehn, E. Rosta, N. J. Russ, S. M. Sharada, S. Sharma, D. W. Small, A. Sodt, *Mol. Phys.* 2015, **113**, 184−215.

7 (a) J. W. Ponder, C. Wu, P. Ren, V. S. Pande, J. D. Chodera, M. J. Schnieders, I. Haque, D. L. Mobley, D. S. Lambrecht, R. A. DiStasio, M, Martin-Gordon, G. N. I. Clark, M. E. Johnson, T. Head-Gordon, 2010, **114**, 2549−2564. (b) N. L. Allinger, F. Li, L. Yan, J. C. Tai, *J. Comput. Chem.* 1990, **11**, 868−895. (c) J. H. Lii, N. L. Allinger, *J. Am. Chem. Soc.* 1989, **111**, 8576−8582.

8 (a) W.-Q. Deng, W. A. Goddard, *J. Phys. Chem. B* 2004, **108**, 8614−8621. (b) Wen, S.-H.; Li, A.; Song, J.; Deng, W.-Q.; Han, K.-L.; Goddard, W. A. *J. Phys. Chem. B* 2009, **113**, 8813−8819.

9 H. Bassler, *Phys. Status. Solidi. B* 1993, **175**, 15−56.

10 R. P. Fornari, A. Troisi, *Phys. Chem. Chem. Phys.* 2014, **16**, 9997−10007.